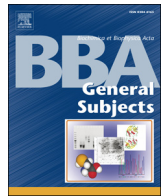




Contents lists available at ScienceDirect

Biochimica et Biophysica Acta

journal homepage: [www.elsevier.com/locate/bbagen](http://www.elsevier.com/locate/bbagen)

# CD1d favors MHC neighborhood, GM<sub>1</sub> ganglioside proximity and low detergent sensitive membrane regions on the surface of B lymphocytes

Q1 Dilip Shrestha<sup>a</sup>, Mark A. Exley<sup>c</sup>, György Vereb<sup>a,b</sup>, János Szöllösi<sup>a,b,\*</sup>, Attila Jenei<sup>a</sup>

<sup>a</sup> Department of Biophysics and Cell Biology, Medical and Health Science Center, University of Debrecen, Nagyerdei krt 98, Debrecen 4032, Hungary

<sup>b</sup> MTA-DE Cell Biology and Signaling Research Group, University of Debrecen, Debrecen, 4032, Hungary

<sup>c</sup> Brigham and Women's Hospital, Harvard Medical School, Boston, MA, USA

## ARTICLE INFO

**Article history:**  
 Received 19 June 2013  
 Received in revised form 15 October 2013  
 Accepted 18 October 2013  
 Available online xxx

**Keywords:**  
 CD1d  
 MHC  
 Rafts  
 FRET  
 Methyl- $\beta$ -cyclodextrin  
 Simvastatin

## ABSTRACT

**Background:** Cluster of differentiation 1 (CD1) represents a family of proteins which is involved in lipid-based antigen presentation. Primarily, antigen presenting cells, like B cells, express CD1 proteins. Here, we examined the cell-surface distribution of CD1d, a subtype of CD1 receptors, on B lymphocytes.

**Methods:** Fluorescence labeling methods, including fluorescence resonance energy transfer (FRET), were employed to investigate plasma membrane features of CD1d receptors.

**Results:** High FRET efficiency was observed between CD1d and MHC I heavy chain (MHC I-HC),  $\beta_2$ -microglobulin ( $\beta_2m$ ) and MHC II proteins in the plasma membrane. In addition, overexpression of CD1d reduced the expression of MHC II and increased the expression of MHC I-HC and  $\beta_2m$  proteins on the cell-surface. Surprisingly,  $\beta_2m$  dependent CD1d isoform constituted only ~15% of the total membrane CD1d proteins. Treatment of B cells with methyl- $\beta$ -cyclodextrin (M $\beta$ CD) / simvastatin caused protein rearrangement; however, FRET demonstrated only minimal effect of these chemicals on the association between CD1d and GM<sub>1</sub> ganglioside on cell-surface. Likewise, a modest effect was only observed in a co-culture assay between M $\beta$ CD/simvastatin treated C1R-CD1d cells and invariant natural killer T cells on measuring secreted cytokines (IFN $\gamma$  and IL4). Furthermore, CD1d rich regions were highly sensitive to low concentration of Triton X-100. Physical proximity between CD1d, MHC and GM<sub>1</sub> molecules was also detected in the plasma membrane.

**Conclusions:** An intricate relationship between CD1d, MHC, and lipid species was found on the membrane of human B cells.

**General significance:** Organization of CD1d on the plasma membrane might be critical for its biological functions.

© 2013 Published by Elsevier B.V.

## 1. Introduction

Antigen presentation is a defining mechanism in the adaptive immune system. While several decades of information are available about peptide antigen presentation, through major histocompatibility complex (MHC) molecules, in the activation of conventional T cells, similar roles of lipids in antigen presentation have gained significant attention beginning only in the last couple of decades [1–3]. The non-polymorphic transmembrane glycoproteins known as Cluster of Differentiation (CD1) were found to present these non-peptide antigens to a distinct subset of T

cells [3,4]. In fact, these CD1 molecules, encoded on human chromosome 1, resemble MHC I heavy chain (MHC I-HC) in physical structure [3,5–7] and MHC II molecules in function, mainly endosomal surveillance [6,8], thus possessing an admixture of features which have led to the hypothesis that these molecules have diverged from a common ancestral gene. Interestingly, MHC I and CD1d also share the chaperones, calnexin and calreticulin, which are important for their appropriate folding [9,10]. In human, CD1 a, -b and -c molecules are placed in group I CD1 while CD1d is kept separately in group II [7,10,11]. CD1d-restricted natural killer T (NKT) cells release copious amount of both Th1 and Th2 type cytokines and chemokines upon engagement with CD1d receptors, underscoring the roles of CD1d in immunoregulation [12,13]. Most earlier studies demonstrated the trafficking behavior of CD1 from the plasma membrane to the intracellular endosomal membrane compartment and vice versa [4,6,14–21]; these studies provided evidence that CD1 molecules sample antigens in the endocytic system but the membrane organization of these receptors which could influence such biological behaviors of these molecules has not been explored in detail yet. Furthermore, owing to the broad role played by CD1d in B lymphocytes, which came into prominence recently due to its role in sustaining antibody responses [22,23] and for the maintenance of invariant natural killer T

**Abbreviations:** MHC, major histocompatibility complex; CD1, cluster of differentiation 1; NKT cells, natural killer T cells; iNKT, invariant natural killer T cells;  $\beta_2m$ ,  $\beta_2$ -microglobulin; M $\beta$ CD, methyl- $\beta$ -cyclodextrin; FRET, fluorescence resonance energy transfer; NCS, newborn calf serum; Mabs, monoclonal antibodies; TfR, transferrin receptor; FCET, flow-cytometric FRET; CTxB, cholera toxin subunit B; FCDR test, flow cytometric detergent resistance test; TX100, Triton X-100; DRMs, Detergent resistant membrane regions; PBMC, peripheral-blood mononuclear cells;  $\alpha$ -gal,  $\alpha$ -galactosylceramide; APC, Antigen presenting cell

\* Corresponding author at: Department of Biophysics and Cell Biology, Medical and Health Science Center, University of Debrecen, Nagyerdei krt 98, Debrecen 4032, Hungary. Tel.: +36 52 412 623; fax: +36 52 532 201.

E-mail address: [szollo@med.unideb.hu](mailto:szollo@med.unideb.hu) (J. Szöllösi).

(iNKT) cells [24], we focused our studies on this molecule, which is also the only CD1 isoform expressed by mouse [7,25]. Two isoforms of CD1d have been observed on the surface of cells: one that is physically bound to  $\beta_2$ -microglobulin ( $\beta_2m$ ) and the other that is independently present without  $\beta_2m$  [11,26]. Hereon, we will address these isoforms as  $\beta_2m$ -dependent and  $\beta_2m$ -independent CD1d proteins. Biochemical studies also illustrated that CD1d is in association with MHC II molecules in the plasma membrane [25] and with invariant chain in membrane-bound intracellular compartments [27]. These observations suggested that these molecules might be in close vicinity of each other and most probably in some specific domains like lipid-rafts. In a murine cell line system, CD1d was distinctly found to be located in the lipid-rafts and the disruption of lipid-rafts by methyl- $\beta$ -cyclodextrin (M $\beta$ CD) was found to interfere with the NKT cell activational responses [28–31]. Furthermore, we reported the co-existence of MHC I and MHC II in nanodomains of various types of cells using fluorescence resonance energy transfer (FRET) [32–36] and electron microscopy [33]. Since, co-immunoprecipitation was mainly used to detect protein–protein interactions in the case of CD1d, even for the membrane fractions, which can present artefactual interactions and is difficult to reproduce, we thought to utilize FRET, which can demonstrate physiological and dynamic interactions and is a better approach to investigate the distribution of CD1d proteins in the plasma membrane. FRET is very sensitive to changes in distance because the rate of energy transfer is inversely proportional to the sixth power of the distance separating the donor and acceptor fluorophores. This sensitivity to distance makes FRET a useful tool for investigating protein–protein interactions within the range of 1–10 nm. In this study, we demonstrate that CD1d proteins are indeed proximal to MHC proteins and are present in detergent sensitive domains of the membrane in lymphocytes. Surprisingly,  $\beta_2m$  dependent CD1d comprised only a small fraction of CD1d proteins on the membrane (~15%). We also noted that CD1d rich regions were mildly affected by cholesterol modulation, but were significantly altered by low concentration of Triton X-100 (TX100). Likewise, a co-culture assay between C1R–CD1d and iNKT cells also demonstrated the partial dependence of CD1d rich regions on cholesterol. In summary, CD1d seems to have an intricate relationship with MHC proteins and membrane lipids, and it also can apparently form larger protein–protein or protein–lipid complexes in the membrane of C1R–CD1d cells.

## 2. Materials and methods

### 2.1. Cell lines

The HLA-C expressing mutant B lymphoid cell line, C1R [37], stably expressing full-length CD1d was used in this study. The characterization of this cell line, including transfection details has been described elsewhere [38]. To obtain cells with uniform CD1d expression, the transfected C1R cells were magnetically sorted using 27.1.9 CD1d antibody and pan anti-mouse secondary antibody conjugated magnetic Dynabeads (Life Technologies/Invitrogen, Budapest, Hungary) following the manufacturer's instructions. Once sorted, the cells were referred to as C1R–CD1d. The cells were grown in RPMI media containing 10% newborn calf serum (NCS), with the inclusion of drug G418 at 300  $\mu$ g/ml concentration unless stated otherwise.

### 2.2. Antibodies

The following monoclonal antibodies (Mabs) were used: the pan-MHC-I W6/32 (recognizes MHC I-HC associated with  $\beta_2m$ , IgG2a) [39,40], HC-10 (recognizes free MHC I-HC, IgG2a) [40–43], L368 (anti- $\beta_2m$ , IgG1) [44], L243 (anti-MHC-DR, IgG2a) [45], OKT9 (anti-transferrin receptor (TfR), IgG1) [46], 51.1.3 (anti-CD1d, IgG2b) and 27.1.9 (anti-CD1d, IgG1) [47]. Antibodies were prepared from hybridoma supernatants according to the standard protocol by Sepharose A affinity chromatography. Antibodies were coupled to Alexa 546- and

Alexa 647-succinimidyl ester dyes following the manufacturer's instructions (Molecular Probes, Invitrogen) and the dye to protein ratios were calculated based on the spectrophotometric absorbance values of the proteins. MEM75 antibody, against TfR [48] was a kind gift from Václav Horejsí (Institute of Molecular Genetics, Academy of Sciences, Prague, Czech Republic).

### 2.3. Cell labeling

For each sample, approximately one million freshly harvested cells were taken in 50  $\mu$ l volume of PBS buffer (pH 7.4) containing 1 mg/ml BSA and 0.01% sodium azide. A saturating concentration of the dye conjugated antibodies was added to these cells, and the mixed suspension was incubated in a dark environment for 30 min on ice. After the incubation, these cells were washed twice with ice-cold PBS buffer in order to remove unbound antibodies. Finally, the cells were suspended in 1% formaldehyde solution, and they were kept at 4 °C until the measurements were performed in a flow cytometer or a confocal microscope.

### 2.4. Quantitation of membrane receptors

In order to determine the expression level of each of the receptors, QIFIKIT (Dako Cytomation, Glostrup, Denmark) was used according to the manufacturer's instructions. QIFIKIT is an indirect immunofluorescence based method of determining antigen density per cell by flow cytometry. This consists of a series of beads coated with known quantities of Mabs which emulate cells with defined antigen densities. Specimen cells were labeled with the primary mouse Mab at saturating concentration. Then, the cells were incubated, in parallel with the QIFIKIT beads, with FITC dye tagged polyclonal anti-mouse secondary F (abs')<sub>2</sub>. Finally, a calibration curve was plotted between the fluorescence intensity of the individual bead populations against the number of Mab molecules on these beads. This curve was then used for determining the number of receptors on the specimen cells by interpolation. For our purpose, fluorescence intensities were measured on a FACScalibur instrument using a 530 +/- 30 BP filter.

### 2.5. Confocal microscopy

A Zeiss LSM 510 confocal laser scanning microscope (Carl Zeiss AG, Jena, Germany) with a Plan-Apochromat 40 $\times$  (NA = 1.2) water immersion objective was used to record the images. An optical slice (512  $\times$  512-pixels) of 1.5  $\mu$ m thickness, four-times averaged, was taken from the top of a cell for co-localization experiments. Simultaneously, a multitrack option of the microscope was used to acquire images to avoid any possible crosstalk between the detection channels.

### 2.6. Co-localization study of the receptors

The spatial proximity of membrane proteins was studied by image cross-correlation method at ~200 nm scale. For this purpose, cells were doubly or triply labeled with markers specific for distinct molecular species but tagged with spectrally different fluorophores. Images were acquired from the top of the cells as a horizontal optical slice by confocal microscope. A custom program written in LABVIEW platform was used for the computational analysis of the cross-correlation coefficient (C) from the image pairs [49,50]. For an image pair 'x' and 'y', the image cross-correlation coefficient was calculated by the following formula:

$$C = \frac{\sum_i \sum_j (x_{i,j} - \langle x \rangle) (y_{i,j} - \langle y \rangle)}{\sqrt{\sum_i \sum_j (x_{i,j} - \langle x \rangle)^2 \sum_i \sum_j (y_{i,j} - \langle y \rangle)^2}}$$

190 where  $x_{ij}$  and  $y_{ij}$  are fluorescence pixel values at co-ordinates  $i$  and  $j$  in  
 192 images  $x$  and  $y$ . Only those pixels that were above the detection thresh-  
 193 old in both images were used for analysis. The theoretical maximum is  
 194 '1' for perfect overlap of proteins (i.e. 100% co-localization); while a  
 195 value '0' implies random overlap of proteins and a negative value '-1'  
 196 indicates an anti-localized situation of the two molecules where a  
 197 pixel is bright in one channel and dim in the other.

## 198 2.7. Flow-cytometric FRET (FCET) experiments

199 FCET experiments were carried out using FACSArray flow cytometer  
 200 (Becton Dickinson, Franklin Lakes, and NJ) equipped with 532 and  
 201 633 nm lasers. For this purpose, samples were either singly or doubly  
 202 labeled with Alexa-546, Alexa-555 or Alexa-647 dye conjugated probes  
 203 and/or antibodies serving as donor and acceptor molecules. Emitted  
 204 signals due to 532 laser excitation were collected in the donor  
 205 (575 +/- 25) and the transfer (650 LP) channels while the 633 nm  
 206 laser excited the acceptor dyes and the signals were collected in the ac-  
 207 ceptor channel (650 +/- 10). The obtained FCS data were analyzed  
 208 using the ReFlex software [51]. The mean FRET efficiencies were then  
 209 calculated from roughly 20,000 cells. For two-color three-protein FCET  
 210 experiment, similar protocol was used as above except the inclusion  
 211 of the third protein as a donor or as an acceptor. The conventional  
 212 FRET has two proteins as a FRET pair but this modified two-color  
 213 three-protein FRET has three proteins as FRET pair, and two of these  
 214 proteins are combinedly used as a donor or acceptor molecules. This  
 215 means two Mabs against two receptors are conjugated to same Alexa  
 216 dyes separately. However, they are mixed during cell-labeling and are  
 217 used as either donor or acceptor. Thus, two Mabs conjugated to same  
 218 Alexa dyes behave together as a unit representing either donor or ac-  
 219 ceptor species.

## 220 2.8. CD1d and GM<sub>1</sub> ganglioside association

221 Cholera toxin subunit B (CTxB) was used to visualize GM<sub>1</sub> ganglio-  
 222 sides and 27.1.9 CD1d Mab was used to identify CD1d proteins. For  
 223 co-localization assay, the experiments were performed using the confo-  
 224 cal microscope as described above, after labeling each of the species in  
 225 the membrane of the cells. Alexa 488 conjugated CTxB was excited by  
 226 488 nm laser and the signals were detected through a 505/550 nm BP fil-  
 227 ter while Alexa 647 conjugated CD1d antibody was excited by 632 nm  
 228 laser and the fluorescence emission was detected through 650 LP filter.  
 229 For the FCET experiment, Alexa 555-CTxB (Invitrogen) was used as a  
 230 donor, while Alexa 647-27.1.9 CD1d Mab was used as an acceptor and  
 231 the measurements were performed in FACSArray.

## 232 2.9. Flow cytometric detergent resistance (FCDR) test

233 For the kinetic assessment of CD1d enriched membrane regions, an  
 234 earlier published protocol based on flow cytometry was followed [52].  
 235 Briefly, cells were labeled with Alexa 488 dyes conjugated Mabs or  
 236 probes in 50  $\mu$ l volume of PBS buffer (pH 7.4) containing 1 mg/ml BSA.  
 237 The incubation and washing of the samples were carried out in a similar  
 238 fashion as described for other samples in the labeling method. Import-  
 239 antly, formaldehyde fixation of cells was not done in this experiment.  
 240 Measurements were carried out immediately after the sample prepara-  
 241 tion using 530 +/- 30 BP filter in FACSscan instrument. At first, fluores-  
 242 cence intensities were recorded without TX100 from all samples  
 243 (~50 s), thereafter, various concentrations of ice-cold TX100 was added  
 244 to the sample swiftly. It was mixed for a few seconds and the measure-  
 245 ments were continued for an additional 5 min. The FCS data were ana-  
 246 lyzed using ReFlex software. Later, SigmaPlot Version 10 was used to  
 247 plot the graph of fluorescence intensity versus time using calculated  
 248 data from ReFlex software.

## 249 2.10. Treatment of cells with methyl- $\beta$ -cyclodextrin (M $\beta$ CD) or simvastatin

250 Simvastatin and M $\beta$ CD were purchased from Sigma, and the solu-  
 251 tions were made as per the instructions from the company. For experi-  
 252 mental purposes, simvastatin was also activated by hydrolysis at  
 253 alkaline pH using sodium hydroxide following the manufacturer's spec-  
 254 ifications. Micromolar ( $\mu$ M) concentration of preactivated simvastatin  
 255 was used to treat 3–10 million cells in 1% NCS RPMI media for 48 h at  
 256 37 °C in a humidified incubator with a constant supply of air with 5%  
 257 CO<sub>2</sub>. For M $\beta$ CD treatment, 5–10 million cells, which were cultured in  
 258 1% NCS, unless otherwise mentioned, were taken in 1 ml of 0.1% NCS  
 259 RPMI media and were incubated with 2 mM M $\beta$ CD for 40 min or  
 260 10 mM M $\beta$ CD for 15 min at 37 °C. Once the incubation was over, in  
 261 both the cases, cells were washed extensively and labeled following  
 262 the protocol described above.

## 263 2.11. Isolation of iNKT cells from peripheral blood mononuclear cells (PBMC)

264 PBMC were isolated from human peripheral blood by standard  
 265 procedure using Ficoll density gradient centrifugation (Sigma).  
 266 Thereafter, iNKT cells were separated from PBMC using human  
 267 anti-iNKT magnetic beads (Miltenyi Biotec, Bergisch-Gladbach,  
 268 Germany). Sorted iNKT cells were grown in flat bottomed 96 well  
 269 plates, which contained  $\alpha$ -galactosylceramide ( $\alpha$ -gal, Avanti Polar  
 270 Lipids, Inc., Alabama, USA) loaded mitomycin-arrested (50  $\mu$ g/ml for  
 271 45 min) C1R-CD1d cells in GIBCO OptiMizer™ CTS™ T-Cell Expansion  
 272 SFM media (Invitrogen). The medium was also supplemented with 5%  
 273 AB human serum (Sera Laboratories International Ltd, West Sussex,  
 274 UK), 200 ng/ml of recombinant IL2 (Shenandoah Biotechnology, Inc.,  
 275 USA) and 2  $\mu$ g/ml phytohemagglutinin M (PHA-M, Sigma). Growth of  
 276 the cells was carefully monitored over the days with clusters of cells in-  
 277 dicating the survival and proliferation of iNKT cells. The concentration  
 278 of IL2 was also gradually decreased from 200 ng/ml to 20 ng/ml  
 279 (~10 U/ml) during the period of culture. The expanded iNKT cells had  
 280 a high purity of >98% when examined by flow cytometry with C21  
 281 (anti-V $\beta$ 11, IgG2a, Beckman coulter), and OKT3 (anti-CD3, IgG2a).

## 282 2.12. iNKT cell activation assay

283 To determine the effect of membrane cholesterol depletion of  
 284 C1R-CD1d cells in iNKT cell activation, a co-culture assay was also de-  
 285 signed. In the case of simvastatin study,  $\alpha$ -gal (250 ng/ml) was added  
 286 to the cells only 4 h prior to the completion of 48 h of simvastatin incu-  
 287 bation, whereas,  $\alpha$ -gal was fed to cells for 18 h in the case of M $\beta$ CD  
 288 study. Cells for simvastatin treatment were grown in 1% NCS RPMI me-  
 289 dium whereas for M $\beta$ CD study were cultured in 10% NCS RPMI medium.  
 290 C1R-CD1d cells were treated either with simvastatin or M $\beta$ CD as de-  
 291 scribed above in the treatment section. Once the reagent treatment  
 292 was over, B cells were fixed with 1% formaldehyde for 20 min on ice  
 293 and were extensively washed, in order to prevent the reassembly of  
 294 cholesterol in the membrane. In the assay, 60,000 C1R-CD1d cells and  
 295 20,000 iNKT cells were seeded in each well of the round-bottomed 96  
 296 well plates with RPMI medium containing 5% human serum and  
 297 20 ng/ml recombinant IL2 for 48 h at 37 °C. Experiments were performed  
 298 in triplicates for each test. Importantly, iNKT cells were grown in 5%  
 299 human serum and 20 ng/ml recombinant IL2 containing RPMI medium  
 300 for at least 48 h before it was used for the experiments.

## 301 2.13. Statistical analysis

302 For comparison, either an unpaired  $t$ -test or one-way ANOVA to-  
 303 gether with Tukey posthoc analysis was performed using SigmaStat  
 304 3.5 (GmbH, Germany) depending on the number of groups. Only ' $p$ '  
 305 values <0.05 were considered significant. Non significant ' $p$ ' values are  
 306 indicated by abbreviation 'N.S.', whereas, ' $p$ ' values <0.05, <0.005, and  
 307 <0.0005 are denoted with \*, \*\*, and \*\*\*, respectively on the figures.

### 3. Results

#### 3.1. Expression level of MHC I-HC, $\beta_2m$ , MHC II and CD1d in C1R-CD1d cells

We wanted to evaluate the relationship between CD1d and MHC molecules on the membrane of B lymphocytes. For this objective, we selected a B lymphoid cell-line, C1R-CD1d which was used in various pull-down experiments previously in an attempt to identify protein interaction partners of CD1d from both plasma membrane and intracellular compartments [10,11,25]. First, we examined the level of expression of various receptors on this cell-line by flow cytometry. As depicted in Fig. 1, MHC II was found to be the highest in expression followed by CD1d while MHC I-HC was almost three and half-fold lower in expression in comparison with MHC II in this cell line. Interestingly, the data obtained from the fluorescently labeled C1R-CD1d cells, after taking into account dyes-to-antibody ratios, also suggested that the membrane expression of  $\beta_2m$  was higher than that of MHC I-HC molecules (Fig. 1).

#### 3.2. Quantitative determination of surface receptors

Fluorescence signals obtained using dye-conjugated antibodies are relative instead of quantitative indicators of the expression level of proteins. Therefore, we calculated the number of MHC I-HC,  $\beta_2m$ , MHC II and CD1d proteins on the membrane of C1R-CD1d cells using QIFIKIT (Fig. 1b). In agreement with the flow cytometric fluorescence histograms, MHC II was found to be the most abundant protein in the membrane of C1R-CD1d cells. Likewise, expression of  $\beta_2m$  was also higher, approximately by 18,000 molecules/cell, in comparison to that of MHC I-HC. MHC I-HC forms a pair with  $\beta_2m$ , a conformation detected by W6/32 antibody [40], and is also known to form self-clusters (oligomers) [33,53]. Therefore, typically the expression of MHC I-HC is higher than that of  $\beta_2m$  proteins in most cells [33]. Hence, in order to identify the possibility of  $\beta_2m$  free unpaired MHC I-HC molecules, we used a HC-10 antibody, which mainly recognizes HLA-B and -C isoforms of  $\beta_2m$  free MHC I [40]. Using these antibodies, we found that there were only a few hundreds of  $\beta_2m$  free MHC I-HC molecules on the surface of C1R-CD1d cells. Similarly, two antibodies, 27.1.9 and 51.1.3 hybridoma clones, against CD1d protein demonstrated comparable surface expression for CD1d proteins (Fig. 1b). Thus, in light of the numerical data, we concluded that  $\beta_2m$  is definitely greater in numbers than MHC I-HC and abundant  $\beta_2m$  independent CD1d is present on the membrane of C1R-CD1d cells.

#### 3.3. CD1d expression affects expression of membrane MHC proteins

During the period of continuous growth, C1R-CD1d cells had the tendency of losing the membrane expression of CD1d; hence, giving rise to CD1d positive (CD1d +ve) and negative (CD1d -ve) population of C1R cells (Fig. 2a). We realized that such a phenomenon can be used to determine the effect of CD1d in the membrane expression of MHC and  $\beta_2m$  proteins. Therefore, we compared the surface expression of these proteins in these two sub-groups. As expected, we observed marked differences in the expression of these proteins in C1R-CD1d “+ve” and C1R-CD1d “-ve” cells.  $\beta_2m$  expression increased significantly in C1R-CD1d “+ve” cells ( $\sim 46.7 \pm 11.5\%$ ) in comparison to that of its expression in C1R-CD1d “-ve” cells thus confirming the role of CD1d in influencing the membrane expression of  $\beta_2m$ . In addition, we also observed an increase in the expression of MHC I-HC ( $\sim 10 \pm 2.6\%$ ) and decrease in the expression of MHC II ( $\sim 31.8 \pm 4.6\%$ ) proteins in the plasma membrane of C1R-CD1d “+ve” in comparison with its C1R-CD1d “-ve” counterparts (Fig. 2b). The comparison of the expression of these proteins between C1R-Mock cells and C1R-CD1d cells also revealed a similar pattern (data not shown).

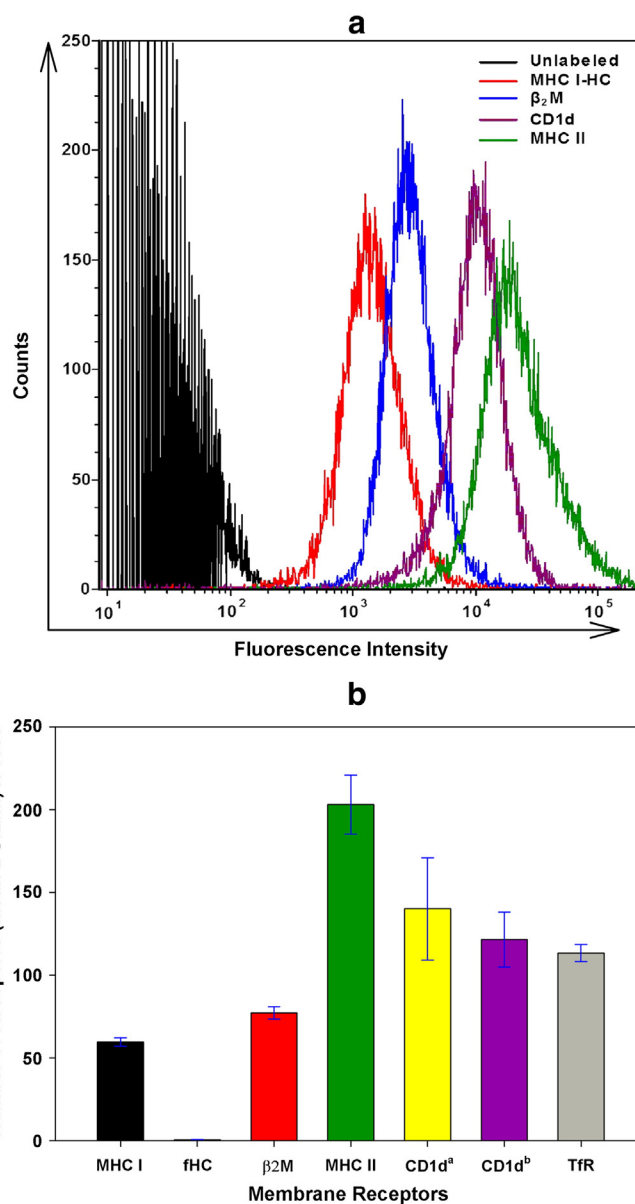
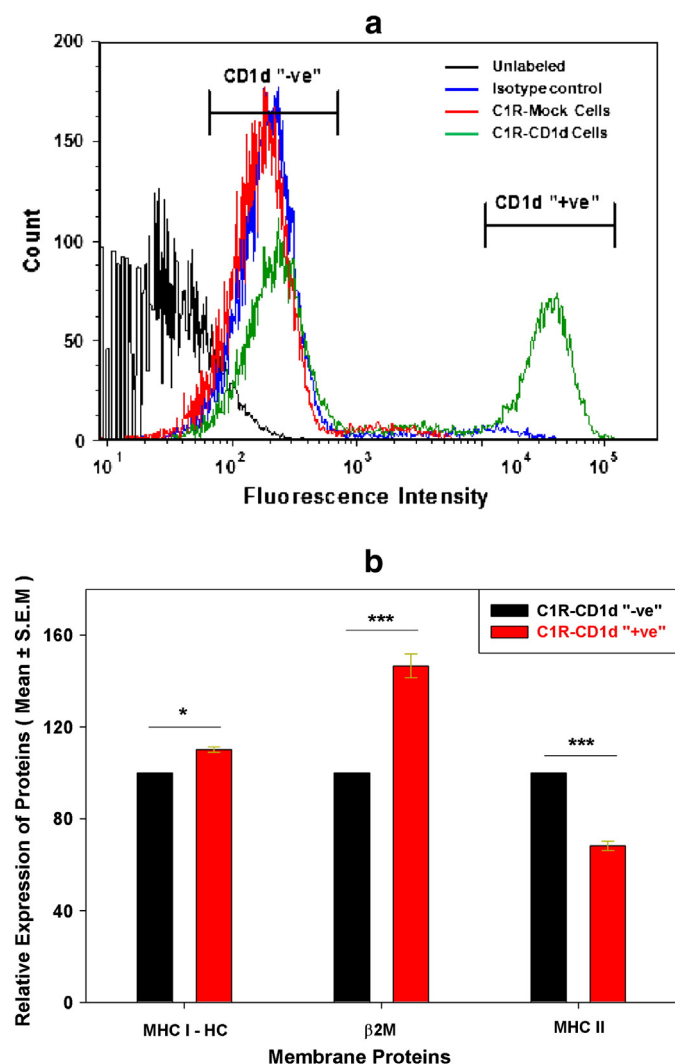


Fig. 1. a) Comparison of expression of various proteins on the surface of C1R-CD1d cells: C1R-CD1d cells were labeled with A647 dye conjugated specific Mabs against MHC I-HC (W6/32) red,  $\beta_2m$  (L368) blue, CD1d (27.1.9 clone) violet, MHC II (L243) green following protocols described in the Materials and methods section independently. Measurements were performed using a FACSAArray flow cytometer. b) QIFIKIT estimation of the number of membrane receptors: Cells were labeled according to the protocols provided by the manufacturer. Briefly, cells were labeled separately with unconjugated antibodies specific for each receptor. The mixture of cells and antibodies were incubated on ice for 30 min. The membrane receptors were saturated with antibodies, then, washing was done using ice-cold PBS buffer. Next, the samples were incubated with FITC conjugated F(ab')<sub>2</sub> for 30 min on ice and in a dark environment. Finally, after washing twice with ice-cold PBS buffer, samples were fixed using 1% formaldehyde. The sample measurements were performed immediately by FACSCalibur. The numbers of receptors are presented as Mean  $\pm$  S.E.M. In the figure, CD1d<sup>a</sup> and CD1d<sup>b</sup> indicate staining of CD1d receptors by 51.1.3 and 27.1.9 CD1d Mabs respectively.

#### 3.4. Co-localization study of MHC I-HC, $\beta_2m$ , MHC II and CD1d in C1R-CD1d cells

Previous studies documented that a lot of common features existed between CD1d and MHC molecules, including antigen presenting characteristics [10,11,25]. Since MHC I and MHC II molecules extensively co-localize in the plasma membrane [32,33,53], we hypothesized that these molecules might be in the vicinity of CD1d as well. Alexa 546 and Alexa 647 dyes conjugated to the same L243 antibody



**Fig. 2.** CD1d expression affects expression of membrane MHC proteins; a) Histograms displaying fluorescence intensities from C1R cells with the following labeling parameters: Unlabeled (Black), Isotype control (Blue), C1R-Mock cells incubated with CD1d antibody (Red) and C1R cells containing C1R-CD1d "+ve" and C1R-CD1d "-ve" cells (Green). A 4D5 antibody, IgG1, against ErbB2 protein – an antigen over expressed in breast cancer cells – was used as an isotype control, where as 27.1.9 CD1d antibody was used to determine CD1d expression in C1R cells. Both the antibodies were conjugated to Alexa 647 dyes. b) The panel shows the change in fluorescence signals in percentage (Mean  $\pm$  S.E.M.) in C1R-CD1d "+ve" population in comparison with a C1R-CD1d "-ve" population. The expression of receptors by C1R-CD1d "-ve" population was taken as 100%. A dual labeling of receptors of interest was carried out simultaneously as described in the **Materials and methods** section. One of the labeled receptors was always CD1d protein while the second receptor was among MHC I-HC,  $\beta$ 2m or MHC II proteins. Measurements were performed by a FACScalibur instrument equipped with blue, 488 nm Ar ion laser, and red, 635 nm diode laser. Positive and negative populations for CD1d protein were gated carefully, and the fluorescence signals for each of the receptors in each population were quantified. Alexa 488 and Alexa 647 dyes conjugated antibodies were used in this experiment to avoid possible spectral overlap between dyes. In the figure, \*, \*\*, and \*\*\* indicate 'p' values <0.05, <0.005, and <0.0005 respectively.

374 were used as a positive control, whereas, GM<sub>1</sub> ganglioside and TfR  
 375 molecules – which are considered to reside in detergent resistant  
 376 and detergent sensitive membrane regions – were used as a negative  
 377 control. On performing a co-localization experiment, we observed  
 378 that several yellow pixels were predominant in the superimposed  
 379 images of CD1d and other proteins (MHC I-HC, MHC II and  $\beta$ 2m)  
 380 resembling a positive control and indicating confinement of these  
 381 proteins in the same regions of the membrane (Fig. 3a). Additionally,  
 382 the cross-correlation coefficient values for these proteins were also  
 383 remarkably high thus confirming the spatial overlap seen in the im-  
 384 ages (Fig. 3b).

### 3.5. Flow-cytometric FRET study among MHC I-HC, $\beta$ 2m, MHC II and CD1d proteins

To substantiate the findings from co-localization studies, which only indicate juxtaposition of molecules, we performed a cell-by-cell FCET which has been described in detail elsewhere [51], to determine the physical associations of CD1d and other proteins (MHC I-HC, MHC II and  $\beta$ 2m). FRET results suggested that MHC I-HC,  $\beta$ 2m and MHC II proteins were physically associated with CD1d (Fig. 4b). In addition, considerably high FRET efficiencies were also observed between these molecular species (Fig. 4a and b). The association of CD1d with  $\beta$ 2m and MHC proteins (MHC I-HC and MHC II) was also detected by acceptor photobleaching FRET (Supplementary Fig. 1). Interestingly, homoassociation FRET results, a FRET occurring between the same receptors when labeled proportionally with mixtures of different conjugates of the same antibody (independent donor and acceptor conjugates), indicated that both CD1d and MHC II molecules could also exist as dimers or oligomers on the surface of these cells. However, the fluorescence signals were not enough to reliably calculate homoassociation FRET for MHC I-HC and  $\beta$ 2m proteins (Fig. 4c).

### 3.6. Association of CD1d with GM<sub>1</sub> gangliosides in C1R-CD1d cells

Peptide antigen presenting MHC molecules are associated with lipid enriched membrane regions also called rafts in various types of cells, including lymphocytes [34,54–57]. In fact, such domains are presumed to facilitate compartmentalization, promote protein–protein and lipid–protein interactions on the cell surface [58] and enhance cellular functions, like antigen presentation [28,30,55]. Therefore, we wanted to determine whether CD1d was also enriched in such lipid regions of the plasma membrane. We probed the relationship between CD1d and GM<sub>1</sub> ganglioside, a frequently used marker for rafts. Our result suggested a high degree of overlap between CD1d and GM<sub>1</sub> gangliosides with a cross-correlation coefficient value of ~0.72. A selected example is presented in Fig. 5a, which demonstrates the overlapping regions of CD1d and GM<sub>1</sub> gangliosides in pink.

### 3.7. Effect of cholesterol depletion and TX100 on CD1d rich membrane regions

The association of CD1d with GM<sub>1</sub> gangliosides was further verified by FRET. Since cholesterol and sphingolipids are the principal components of plasma membrane, we also tested the effect of cholesterol depletion on the observed association between CD1d and GM<sub>1</sub> gangliosides. Simvastatin, a cholesterol synthesis inhibitor [59], and methyl- $\beta$ -cyclodextrin (M $\beta$ CD), a known membrane cholesterol extractor from the cell [60], was considered for this purpose. At resting state, a significant FCET result, proving a distinct association, was obtained between CD1d and GM<sub>1</sub> gangliosides. Interestingly, treatment of cells with either M $\beta$ CD or simvastatin appeared to have a minor effect on the association of CD1d with GM<sub>1</sub> subunits, the effect was not significant at the used concentrations of reagent based on our study (Fig. 5b). Therefore, we performed FCDR experiments to further characterize these CD1d rich regions using detergent TX100. We noted that CD1d rich regions were very sensitive to low concentration of TX100 as depicted in Fig. 6d. Surprisingly, TfR, a non-raft marker abundant in non detergent resistant membrane regions (DRMs) (see also Supplementary Fig. 2), fared better than CD1d in terms of tolerance to TX100 (Fig. 6c and d). MHC II proteins, which are known to partially reside in DRMs, demonstrated superior resistance to TX100 than by TfR proteins (Fig. 6b, c and e). Likewise, the raft marker GM<sub>1</sub> molecules were resilient to TX100 treatment at the employed concentrations. The tolerance to TX100 for these molecules was in the following order: GM<sub>1</sub> > MHC II > TfR > CD1d (Fig. 6). At a typical concentration of 0.013% TX100, the fluorescence intensities of CD1d decreased to ~15%, TfR decreased to ~70%, MHC II decreased to ~80% and

446 that of GM<sub>1</sub> decreased to ~95% within 3 min (Fig. 6e). The maximal decline in fluorescence intensity was observed for CD1d among all tested  
447 surface markers. Therefore, mild detergent sensitivity is a specific feature  
448 of CD1d proteins on the membrane of B lymphocytes.  
449

### 3.8. Effect of M $\beta$ CD and simvastatin on C1R–CD1d cells in iNKT cell activation

450 Studies, primarily based on murine cell lines have demonstrated  
451 contrasting relationships of CD1d with rafts in the plasma membrane.  
452 One of the studies suggested that raft localization of CD1d in antigen  
453 presenting cells (APCs) is essential for signaling through TCR of NKT  
454 cells [28] while another study suggested only a modest effect in the  
455 CD1d mediated antigen presentation ability [61] due to M $\beta$ CD treat-  
456 ment of APCs. Owing to these discrepancies, we performed similar ex-  
457 periments but on human cell lines using primary iNKT cells. We also  
458 determined the consequences of simvastatin treatment of B cells on  
459 the activation of iNKT cells. We observed that application of 10 mM  
460 M $\beta$ CD (15 min) to C1R–CD1d cells reduced the membrane expres-  
461 sion of CD1d proteins ( $28.8 \pm 2.3\%$ , Mean  $\pm$  S.E.M) in C1R–CD1d  
462 cells (Supplementary Fig. 3a); however, this was accompanied by a  
463 greater decrease in the production of both cytokines (IFN $\gamma$  up to 42%  
464 and IL4 up to 33%) from iNKT cells. Two millimolar M $\beta$ CD did not  
465 lower the expression of CD1d in C1R–CD1d cells at the used condition  
466 and it had only a modest inhibitory effect on the release of IFN $\gamma$  and  
467 IL4 by iNKT cells. Interestingly, the reduction in cytokine production  
468 was more prominent in the case of smaller concentration of  $\alpha$ -gal  
469 (Fig. 7a and b). Furthermore, despite reports on the negative effect of  
470 simvastatin in APCs in reducing the cytokine release by iNKT cells  
471 [61], we observed that either there is no effect or slight up regulation  
472 of cytokines (IL4 and IFN $\gamma$ ) by human iNKT cells upon  
473 treatment of human C1R–CD1d cells with simvastatin (Fig. 7c and d).  
474  
475

### 3.9. Simvastatin and M $\beta$ CD alter membrane protein distribution

476 Biological membranes are semi-fluid in nature with cholesterol  
477 playing a major part in maintaining the integrity of the membrane.  
478 Because, cholesterol affects fluidity and bending stiffness of the mem-  
479 brane, we expected alterations in the membrane protein distribution  
480 of C1R–CD1d cells when treated with M $\beta$ CD and simvastatin. We  
481 found that both compounds had an effect on the topological arrange-  
482 ment of these proteins in the plasma membrane which means that the  
483 drugs had relevant effects on the cell. As demonstrated in Fig. 8, we  
484 observed changes in FRET efficiency between CD1d and MHC proteins,  
485 especially in the case of simvastatin. Interestingly, the association of  
486 MHC I-HC to  $\beta_2m$  is significantly altered in both the cases. Changes in  
487 FRET efficiencies between the proteins complemented the observed ef-  
488 fect in the decrease of CD1d expression in the cells due to the treatment  
489 of these compounds ( $25.2 \pm 1.9\%$ , Mean  $\pm$  S.E.M, decrease in membrane  
490 CD1d expression due to 10  $\mu$ M simvastatin, Supplementary Fig. 3b).  
491 Therefore, both compounds alter the distribution of membrane proteins  
492 on the surface of C1R–CD1d cells.  
493

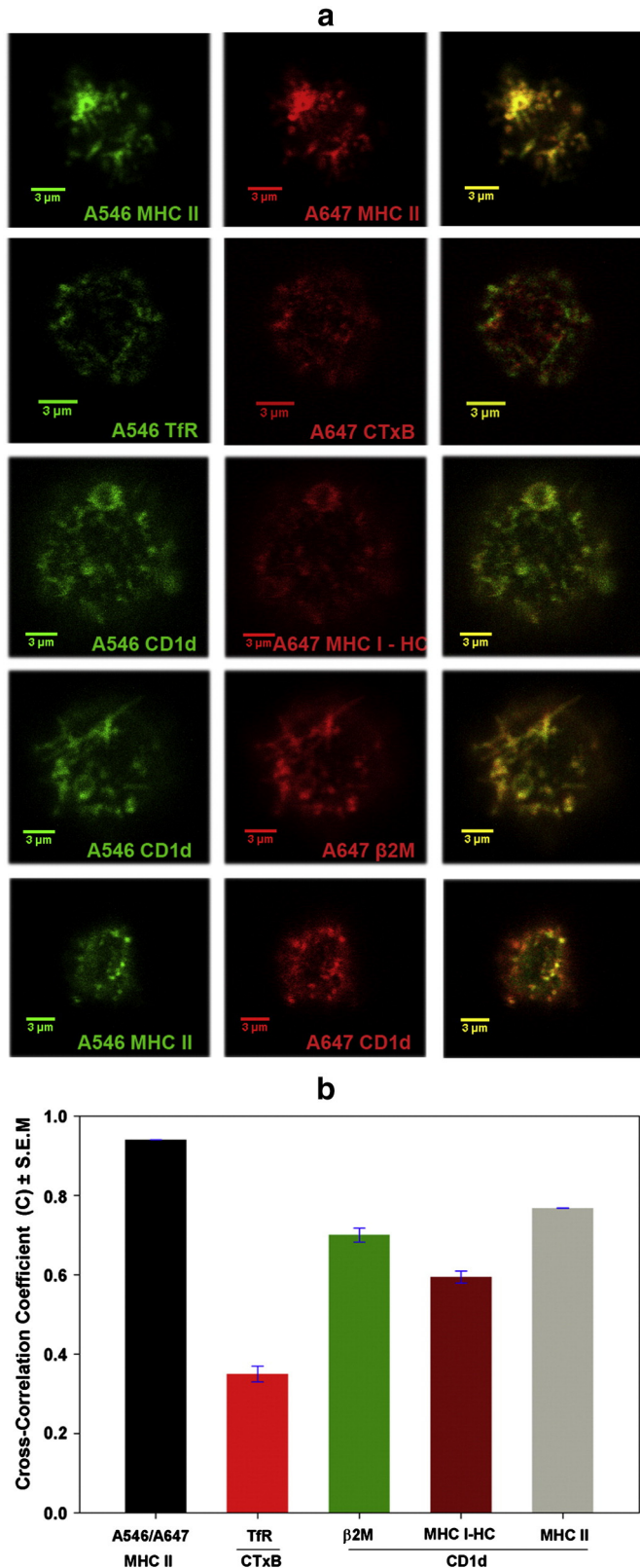


**Fig. 3.** Co-localization of receptors: Representative images for each of the receptors used in co-localization study are presented here. Images at 1.5  $\mu$ m thickness were scanned from the top of the membrane of a cell. The images were background subtracted in this figure. The first two columns in green and red indicates the images of two different molecular species in pseudo color taken in two different channels of the microscope, and the third column represents the superimposed image for these two channels. The name of the molecules which were imaged is shown on the bottom right corner of each image. Emission from Alexa 546 and Alexa 647 dyes were collected through 560/615 nm BP filter and 650 LP filter respectively. a) Cells were labeled with antibodies against each of the receptors denoted at the x-axis according to the steps described in the Materials and methods section. Thereafter, the top of the membrane was used to record numerous images for each sample from several cells. Next, the co-localization of the two receptors in question was calculated in terms of cross-correlation coefficient value using the LabView program. The first and second row columns indicate positive and negative control respectively. The other columns show the 'C' values between CD1d and other molecules that were probed together. The specific dye conjugated antibodies used are mentioned on the right bottom of each image in Fig. 3a. For a positive control, the same L243 antibody was conjugated with both Alexa 546 and Alexa 647 dyes while CTxB and TfR molecules were used for negative controls.

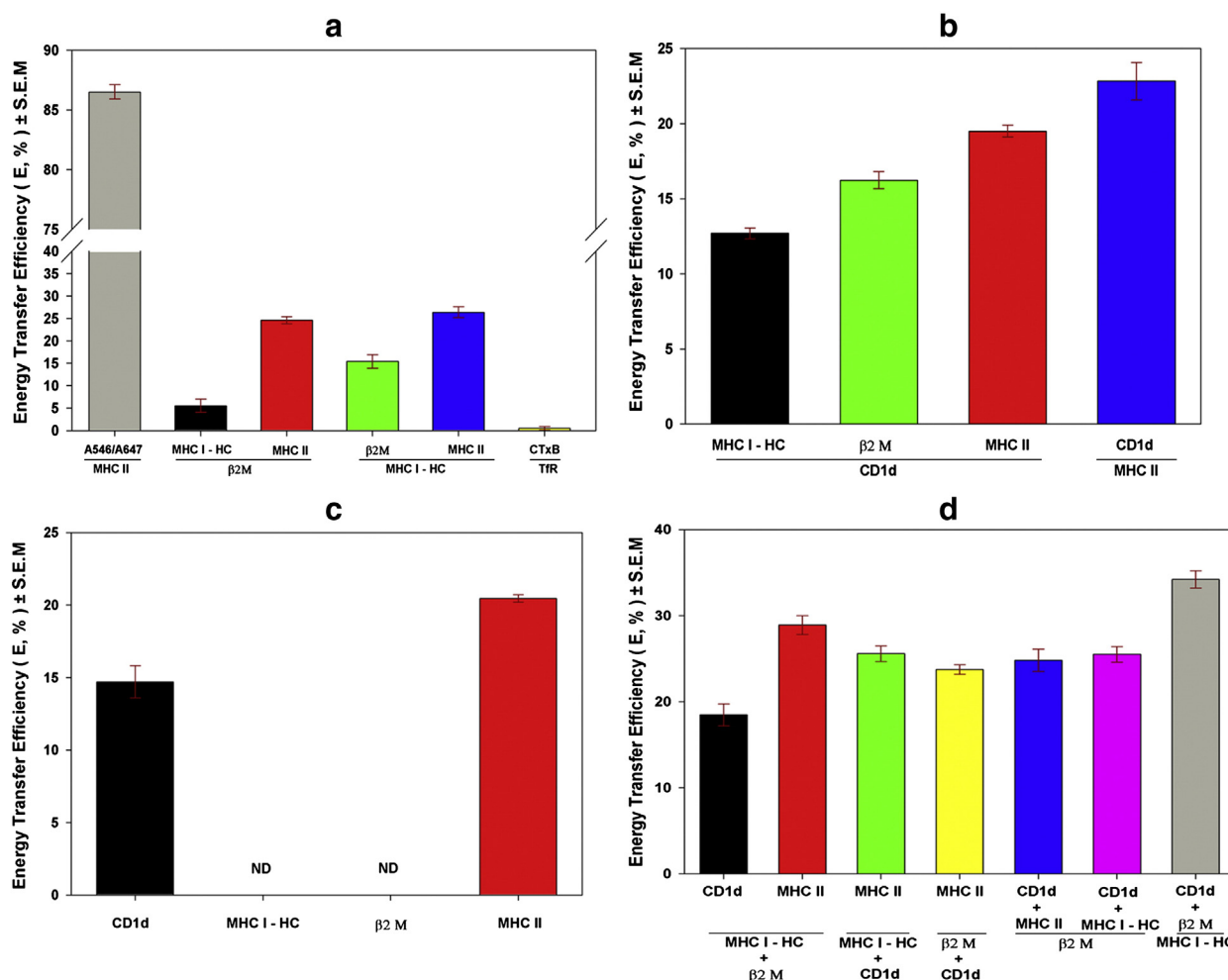


**Fig. 4.** Flow cytometric FRET (FCET). A) Flow cytometric FRET between the proteins: Columns from left to right represent: Positive Control (Gray) – Both A546 and A647 dyes were conjugated to the same L243 antibody;  $\beta$ 2m served as a donor while MHC I-HC (Black) or MHC II (Red) served as an acceptor; MHC I-HC served as a donor while  $\beta$ 2m (Green) or MHC II (Blue) served as an acceptor; CTxB served as a donor while TIR served as an acceptor (Yellow). The FRET pair was always Alexa 546 and Alexa 647 dyes conjugated Mabs except for negative control where CTxB probes were conjugated with Alexa 555 dyes and were used as donor. Flow cytometric FRET between the proteins: b) Columns from left to right represent: CD1d served as an acceptor while MHC I-HC (Black) or  $\beta$ 2m (Green) or MHC II (Red) served as a donor; MHC II served as an acceptor while CD1d (Blue) served as a donor) Homoassociation Flow cytometric FRET between the proteins: The proteins are described in the x-axis. r.d) Flow cytometric FRET among three proteins: Columns from left to right represent: (MHC I-HC +  $\beta$ 2m) served as a donor while CD1d (Black) or MHC II (Red) served as an acceptor; (MHC I-HC + CD1d) served as a donor while MHC II (Green) served as an acceptor; ( $\beta$ 2m + CD1d) served as a donor while MHC II (Yellow) served as an acceptor;  $\beta$ 2m served as a donor while (CD1d + MHC II) (Blue) or (CD1d + MHC I-HC) (Pink) served as an acceptor; MHC I-HC served as a donor while ( $\beta$ 2m + CD1d) (Gray) served as an acceptor. (Note: Proteins with '+' mark means the Mabs against these receptors were conjugated to same Alexa dyes. For example 'MHC I-HC +  $\beta$ 2m' means Mabs against MHC I-HC and  $\beta$ 2m were conjugated to Alexa 546 independently and were used in combination as donors for FRET. The same case is also true for two proteins when used as acceptors except that the Mabs against proteins were conjugated to Alexa 647 dyes.)

### 3.10. Multimolecular complexes of CD1d, MHC and lipid species on the membrane of C1R-CD1d cells

We had no doubts that CD1d and both MHC molecules were associated with each other on the surface of C1R-CD1d cells. Therefore, we assumed that perhaps these molecules can also form a multimolecular protein complex in the membrane of these cells. To demonstrate such possibilities, we performed triple co-localization experiments. The co-occurrence of these proteins was clearly visible, as white pixels, on the superimposed images. Likewise, overlapping regions were also noticed when two of these proteins were imaged together with GM<sub>1</sub> ganglioside (Fig. 9). However, the differential propensity of enrichment in GM<sub>1</sub> rich regions was found between MHC I and MHC II proteins. FRET and co-localization demonstrated that MHC I-HC had a very weak association with GM<sub>1</sub> subunits in comparison with MHC II receptors (Fig. 9, Supplementary Fig. 2 and Supplementary Table 1). Triple co-localization of proteins demonstrating trimolecular complexes of proteins was also supported by our two-color but three-protein FCET experiment. Such a modified FRET setup would help to predict the

possibilities of trimolecular complexes in comparison with the conventional two-protein FRET pair which only suggests the interaction of two proteins. With this modified scheme, the FRET efficiency should increase between two proteins in comparison with conventional two protein FRET system when a new protein which is generally a part of trimolecular complex is also included in the FRET pair. In accordance with such assumptions, we observed an increase in the FRET efficiency between any two proteins with the inclusion of a third protein mainly with MHC II as acceptor (Fig. 4d). Thus, considering all lines of evidence, we conclude that multimolecular complexes of CD1d and other proteins (MHC I-HC,  $\beta$ 2m and MHC II) are present in the plasma membrane of these cells, preferably but not exclusively in non-GM<sub>1</sub> regions.

## 4. Discussion

Non-random distribution patterns of MHC I and MHC II proteins in the plasma membrane have been described in various cell types [32,33,35,36,53,54,56,62]. The modification of these proteins organization was also found to occur during several physiological events, for

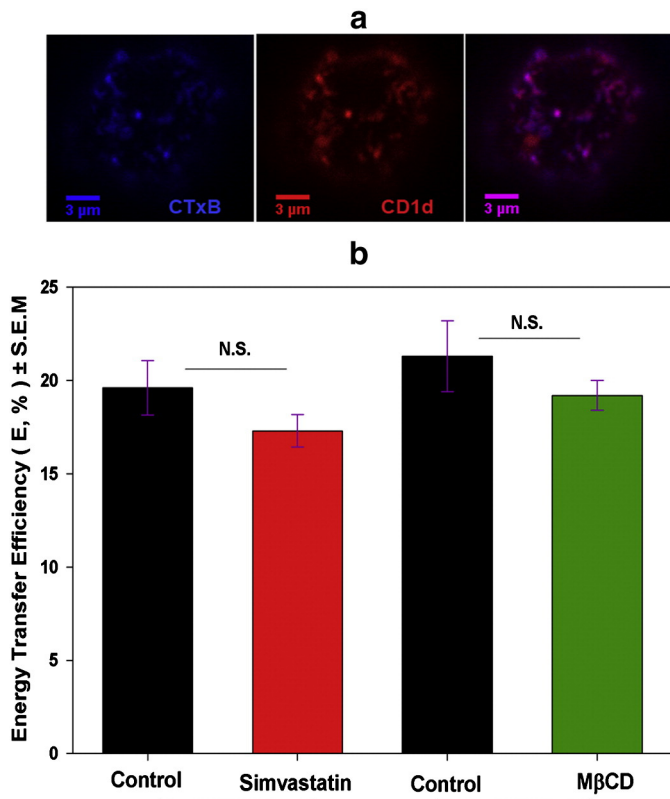


**Fig. 5.** CD1d and GM<sub>1</sub> ganglioside co-localization: a. Representative image of the distribution of CD1d and GM<sub>1</sub> ganglioside. GM<sub>1</sub> gangliosides were labeled with Alexa 488-CTxB (Blue) and CD1d was labeled with Alexa 647–27.1.9 (Red). The overlay image is presented in the third column with pink pixels indicating co-localization. b) Effect of MβCD and Statin in the Relationship between CD1d and GM<sub>1</sub> ganglioside: C1R–CD1d cells were treated with MβCD and simvastatin as described in the **Materials and methods** section. Thereafter, the cells were labeled with saturating concentrations of CD1d antibodies and CTxB molecules for FRET experiments. CTxB was used as a donor while CD1d protein was used as an acceptor for FRET. Statistically non-significant 'p' value is indicated as "N.S." in the figure.

example during immune synapse formation [63,64], diseased condition [65] and cell differentiation stages [66]. However, to our knowledge, no such report is present till now that has demonstrated the quiescent state distribution of CD1d protein in the plasma membrane of B cells. Therefore, using biophysical approaches – including FRET – for the first time we have documented the resting state topological features of CD1d in the plasma membrane of B cells in this study. Quantitative estimation of the number of membrane proteins and evaluation of FRET efficiencies between various protein pairs helped us derive the proximity relationship among MHC I-HC,  $\beta_2m$ , MHC II, and CD1d proteins. We found that CD1d receptors were physically close to MHC I-HC,  $\beta_2m$  and MHC II proteins on the cell-surface. Though the physical association of  $\beta_2m$  and CD1d is not a new phenomenon, our data suggest that the proximity between these two proteins is not entirely dependent on the known non-covalent interactions / or direct binding of these proteins. Rather, the physical association between MHC I and CD1d can also spatially position  $\beta_2m$ , which are mostly bound to MHC I, closer to CD1d proteins (Fig. 4). Since both MHC I-HC and CD1d can interact with  $\beta_2m$  proteins, expectedly there was higher  $\beta_2m$  (~40%) in the plasma membrane of C1R–CD1d "+ve" cells in comparison with C1R–CD1d "-ve" cells. However, flow-cytometric

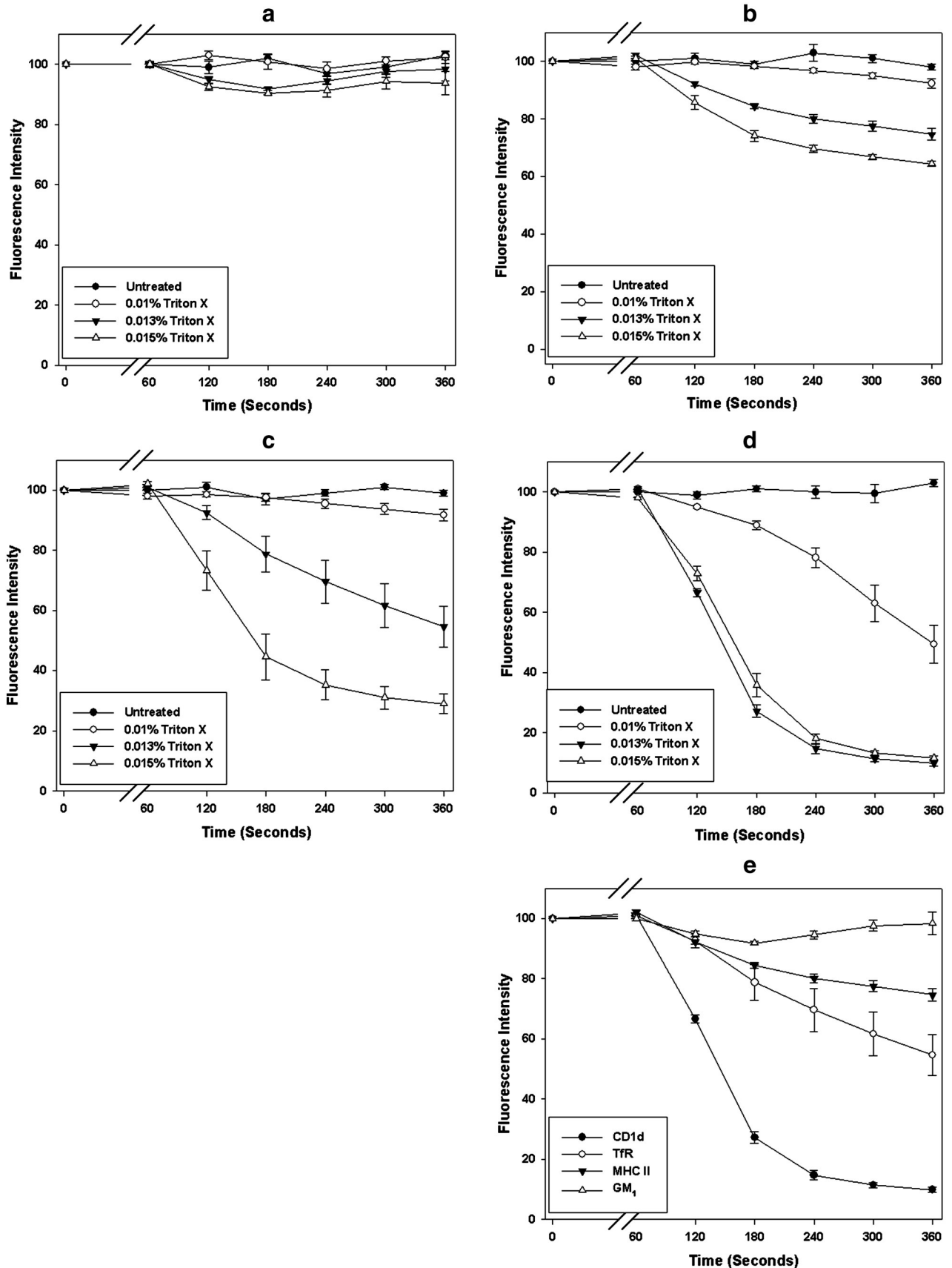
fluorescence histograms and quantitative estimation of membrane proteins in C1R–CD1d "+ve" cells indicated that the total number of  $\beta_2m$  was about 60% of the CD1d proteins expressed in the surface of these cells. Furthermore, almost the entire MHC I-HC (>99%) population was in non-covalent interaction with  $\beta_2m$  based on HC-10 and W6/32 staining of MHC I protein in C1R–CD1d "+ve" cells (Fig. 1b). Therefore, the enhanced number of  $\beta_2m$  in the plasma membrane of C1R–CD1d "+ve" cells represents the only fraction of CD1d that is directly bound with  $\beta_2m$  (~15% of membrane CD1d proteins). The occurrence of very high FRET efficiency between  $\beta_2m$  and CD1d, MHC I-HC and CD1d, MHC II and CD1d proteins also strongly implies that these proteins are the constituents of the same multiprotein complexes. The presence of such supramolecular complexes should also explain why  $\beta_2m$  demonstrated high FRET efficiency with CD1d despite a small fraction of these proteins being bound to CD1d directly (~15%). It thus advances the notion that most of the CD1d (~85%) on the surface of C1R–CD1d cells are not directly bound to  $\beta_2m$ . This might represent the population of CD1d which is immature/ or with poor glycosylation modifications. This observation also complements the earlier reports in which these two isoforms were described by biochemical methods [11,67]. Of note, we did not observe any fluorescence staining due to C3D5 Mab, an antibody considered to bind only CD1d heavy chain, on the plasma membrane of C1R–CD1d cells (Data not shown). The inability of this Mab to bind surface CD1d proteins has been noted before [47,68]. This suggests that 27.1.9 and 51.1.3 Mabs can bind both isoforms of CD1d on the cell surface and the non-binding of C3D5 to plasma membrane CD1d proteins rather indicates the inability of C3D5 Mab to recognize the conformation of CD1d heavy chain on the plasma membrane or masking of the epitope recognized by C3D5 or presence of steric hindrance due to multimolecular complexes of proteins on the cell surface. Thus, it remains a challenge to correctly predict the level of expression of both isoforms of CD1d ( $\beta_2m$ -dependent and  $\beta_2m$ -independent forms of CD1d) on the plasma membrane. Nevertheless, both isoforms have been identified in mouse B cells and are found to be capable of activating T cells [69]. It is possible that both isoforms may have distinct functional roles in the activation of T cells. CD1d receptors also displayed homoassociation FRET, suggesting that CD1d proteins can also exist as self clusters in the plasma membrane. Previously, atomic force microscopy (AFM) recognition imaging has revealed the existence of self clusters of CD1d in the plasma membrane of THP1 monocytic cells [70,71]. However, AFM imaging of these cells was carried out in lipid ligand activated monocytic cells. Furthermore, iNKT TCRs were used to investigate CD1d receptors on the plasma membrane. Lipid loading on dendritic cells was found to induce the entry of CD1d receptors to DRM regions [30], therefore, the AFM study should have detected the modified distribution of CD1d receptors unlike the resting state distribution of CD1d receptors. The changes in the plasma membrane distribution of CD1d receptors on lipid loading is also corroborated by the observation that two different lipid antigens produced two different patterns of CD1d distribution on the plasma membrane of THP1 cells [71]. Furthermore, TCRs could only identify lipid bound CD1d receptors. Hence, our study with a specific Mab (27.1.9 clone) which can detect individual CD1d receptors, with or without lipids, is a representation of the quiescent state distribution of CD1d receptors in B cells. We also examined the propensity of CD1d towards lipid species using GM<sub>1</sub> ganglioside at quiescent state. Co-localization and FRET studies indicated the preference of GM<sub>1</sub> rich regions by CD1d proteins. However, cholesterol depleting agents, MβCD and simvastatin, had only a modest effect on the association of CD1d with GM<sub>1</sub> species based on FRET. Plasma

**Fig. 6.** Flow cytometry based detergent resistance analysis: The response of various surface molecules to TX100 treatment is presented as fluorescence intensity versus time. The samples were prepared by incubating cells with respective probes independently (see **Materials and methods** also). Non-fixed samples were processed for the measurements. Signals from the TX100 untreated samples were measured for approximately 50 s, then, ice-cold TX100 at various concentrations (untreated, 0.01%, 0.013% and 0.015%) was added to the samples, thereafter, the measurement was continued for approximately 5 min. a) GM<sub>1</sub> subunits b) MHC II proteins c) TfR d) CD1d proteins e) GM<sub>1</sub>, MHC II, TfR and CD1d species at 0.013% TX100. The fluorescence intensities were averaged for every 60 seconds except for the first minute where it was averaged for 45 s. The break in the graph (from 45 to 50 s) represents the point of addition of TX100 except for untreated samples where continuous measurements for 6 min were performed. The data for each value is calculated from at least three sets of independent experiments and is presented as Mean ± S.E.M.



609 membrane cholesterol level decreased by greater than 30% due to both  
 610 chemicals when monitored by filipin staining (data not shown). These  
 611 chemicals also alter the topological distribution of membrane proteins

(Fig. 8). Therefore, CD1d rich regions show proximity to GM<sub>1</sub> regions  
 612 and only partial dependence on cholesterol. The observation with  
 613 MβCD is straightforward because it specifically removes the cholesterol  
 614



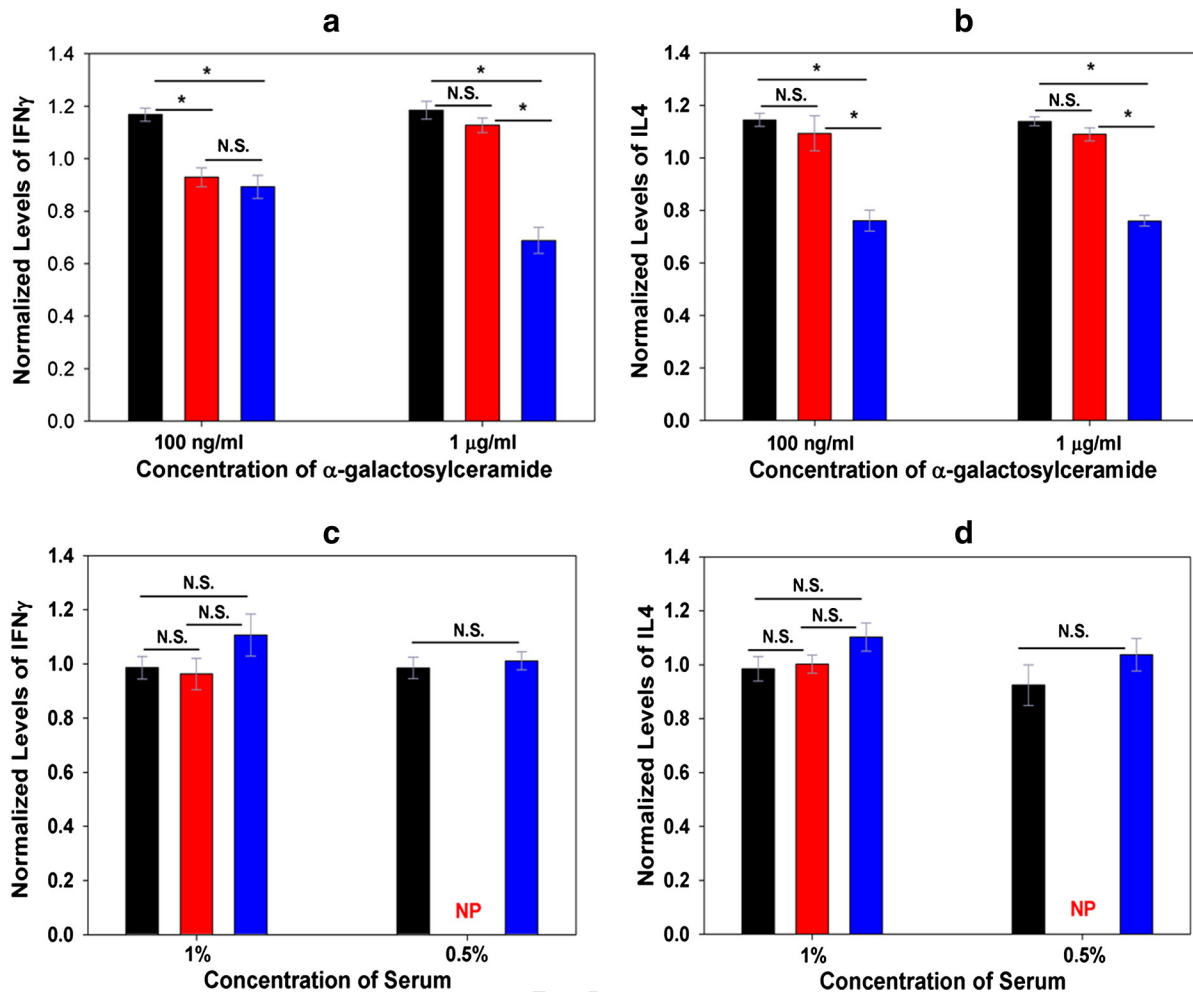


**Fig. 7.** Effect of M $\beta$ CD and simvastatin on C1R–CD1d cells in terms of iNKT cell cytokines release: For statistical analyses, either one-way ANOVA together with tukey post-hoc analyses or unpaired *t*-test was done. Statistically non-significant and significant ( $p < 0.05$ ) values are indicated by N.S. and '\*' symbols respectively. Each datum was normalized by the averaged sum of all data-sets of the particular independent experiment, including values from both control and treated samples, and is represented as Mean  $\pm$  S.E.M. Three or more independent experiments in triplicates were performed for this study. a. Measurement of IFN $\gamma$  in the medium after 48 h of co-culture between C1R–CD1d cells and iNKT cells. C1R–CD1d cells were loaded with either 100 ng/ml or 1  $\mu$ g/ml  $\alpha$ -gal for 18 h thereafter it was washed and treated with M $\beta$ CD. Next, samples were fixed with 1% formaldehyde for 20 min in ice before being used in the co-culture assay. The samples are indicated by the columns in the following colors: Control (Black); 2 mM M $\beta$ CD treated (Red); 10 mM M $\beta$ CD treated (Blue). The amount of IFN $\gamma$  in control samples in Mean  $\pm$  S.E.M were 1589  $\pm$  402 pg/ml (100 ng/ml  $\alpha$ -gal culture) and 1642  $\pm$  412 pg/ml (1  $\mu$ g/ml  $\alpha$ -gal culture). b. Measurement of IL4 in the medium after 48 h of co-culture between C1R–CD1d cells and iNKT cells. C1R–CD1d cells were loaded with either 100 ng/ml or 1  $\mu$ g/ml  $\alpha$ -gal for 18 h thereafter it was washed and treated with M $\beta$ CD. Next, samples were fixed with 1% formaldehyde for 20 min in ice before being used in the co-culture assay. The samples are indicated by the columns in the following colors: Control (Black); 2 mM M $\beta$ CD treated (Red); 10 mM M $\beta$ CD treated (Blue). The amount of IL4 in control samples in Mean  $\pm$  S.E.M were 551  $\pm$  153 pg/ml (100 ng/ml  $\alpha$ -gal culture) and 604  $\pm$  109 pg/ml (1  $\mu$ g/ml  $\alpha$ -gal culture). c. Measurement of IFN $\gamma$  in the medium after 48 h of co-culture between simvastatin treated C1R–CD1d cells and iNKT cells. C1R–CD1d cells were incubated for 48 h with simvastatin (10  $\mu$ M, Red and 20  $\mu$ M, Blue) or without simvastatin (Black) either in 1% NCS media or 0.5% NCS media. Four hours prior to the completion of this incubation period, 250 ng/ml  $\alpha$ -gal was added to the C1R–CD1d cells for the loading of iNKT ligand. Next, C1R–CD1d cells were washed extensively and were fixed in 1% formaldehyde for 20 min on ice. Only fixed C1R–CD1d cells were used in the co-culture assay. Experiment with 10  $\mu$ M simvastatin treatment of C1R–CD1d cells was not performed for 0.5% NCS group. 'NP' means 'Not Performed' in the figure. The amount of IFN $\gamma$  in control samples in Mean  $\pm$  S.E.M were 1542  $\pm$  407 pg/ml (1% NCS culture) and 2407  $\pm$  337 pg/ml (0.5% NCS culture).

628 from the plasma membrane, however, the effect of simvastatin might  
 633 be due to its impact on both cholesterol reduction and isoprenoid path-  
 634 way. Justifying the secondary effects of simvastatin, it has been reported  
 635 earlier that simvastatin could decrease antigen presentation by MHC II  
 636 proteins independent of its inhibitory role in the cholesterol biosynthe-  
 637 sis [72]. Here, we also observed an increase in GM $_1$  surface expression  
 638 due to simvastatin treatment (Data not shown), further indicating it's  
 639 another secondary effect. The partial dependence of CD1d rich regions  
 640 on cholesterol is also reflected by the co-culture assay between  
 641 M $\beta$ CD/simvastatin treated C1R–CD1d cells and iNKT cells. Even on feed-  
 642 ing the C1R–CD1d cells with the lipid ligand,  $\alpha$ -gal, which induces mi-  
 643 gration of CD1d to DRM regions, treatment of C1R–CD1d cells with  
 644 M $\beta$ CD lead to only a modest decrease in cytokine secretion by iNKT  
 645 cells. This could be correlated with the partial dependence of CD1d  
 646 rich regions on cholesterol in the plasma membrane. However, the situ-  
 647 ation appears to be different for simvastatin because we did not see

any decrease, rather observed a slight upregulation, in cytokine secre- 648  
 tion by iNKT cells despite reduction in the membrane expression of 649  
 CD1d in C1R–CD1d cells. Simvastatin decreases the level of membrane 650  
 cholesterol (more than 30% reduction in cholesterol, data not shown) 651  
 and induces rearrangement of proteins in the plasma membrane. It 652  
 also seems to affect the expression level of proteins/lipids in the plasma 653  
 membrane which can modify the fluidity of the membrane. Likewise, 654  
 simvastatin has been reported to alter the function of small GTPases 655  
 [73–76] and was also found to disrupt the actin cytoskeleton [77,78] 656  
 in numerous studies. Actin destabilizing agent and Rho kinase inhibitors 657  
 were found to enhance antigen presentation by CD1d in murine cells 658  
 [79]. Therefore the effects of simvastatin on antigen presentation due 659  
 to decrease in CD1d membrane expression and cholesterol depletion 660  
 could have been negated by the ability of simvastatin to alter other 661  
 biological functions including modification of Rho kinase functions 662  
 and disruption of actin cytoskeleton. However, it would need further 663

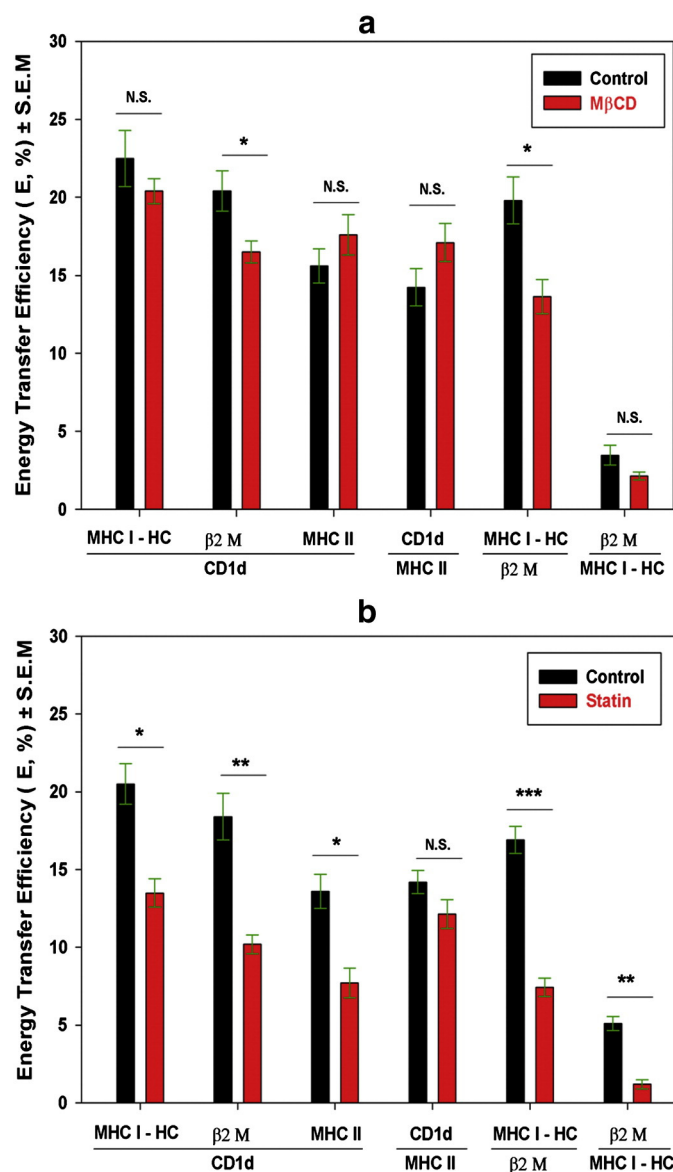


**Fig. 8.** MβCD and Simvastatin alter membrane protein distribution: C1R–CD1d cells were treated with either MβCD (2 mM, 40 min) or simvastatin (10 μM, 48 h) according to the optimized protocol (Materials and methods). Thereafter, the samples were prepared for FRET experiments accordingly. In the figure, statistically non-significant 'p' value is indicated as 'N.S.', whereas 'p' values <0.05, <0.005, and <0.0005 are indicated by \*, \*\*, and \*\*\* symbols respectively. a) FRET values for control samples are in black while MβCD treated samples are in red colors. Proteins mentioned below the ticks in x-axis served as a donor while the one that is under the common line served as acceptor for the FRET experiments. b) FRET values for control samples are in black while simvastatin treated samples are in red colors. Proteins mentioned below the ticks in x-axis served as a donor while the ones that are under the common line served as an acceptor for the FRET experiments.

cholesterol containing plasma membrane regions [54] which reflects the feature of CD1d rich regions, however, unlike MHC I which is very weakly associated with GM<sub>1</sub> gangliosides, CD1d shows strong GM<sub>1</sub> association, a feature of MHC II proteins. Earlier studies based on various detergents analyses also reinforce the notion that different types of rafts/ or detergent resistant membrane regions might exist [54,81,82]. In addition, recently cholesterol independent sphingolipid domains, ~200 nm in diameter, were highlighted in the plasma membrane of fibroblasts. These sphingolipid domains were primarily dependent on underlying cytoskeletal structures rather than cholesterol [83]. Thus, the nature of CD1d enriched membrane regions needs further characterization especially by comparing it with MHC enriched domains and other raft like domains. Remarkably MHC I, MHC II and CD1d species also demonstrated strong co-occurrence in the plasma membrane. Furthermore, MHC II and CD1d showed markedly high presence in GM<sub>1</sub> rich regions, whereas, MHC I and CD1d scantily co-distributed in GM<sub>1</sub> regions (Fig. 9). Therefore, these molecules as a supramolecular complex are present in the plasma membrane although differences might occur in the abundance of these clusters in GM<sub>1</sub> rich or non-GM<sub>1</sub> rich regions. While unraveling the surface organization features of CD1d receptors, we also found that the plasma membrane expression of CD1d would affect the surface expression of MHC proteins. Since CD1d shares chaperones and invariant chain with MHC proteins, the observed effect might be related to the competition among these proteins for these shared proteins in the intracellular compartments. Such assumption is supported by the fact that cells from invariant chain deficient mice have comparatively low cell surface expression of MHC II proteins and decreased antigen presentation capacity than from normal mice [84,85]. Likewise, expression of CD1a, a subtype of CD1 protein increases the expression of invariant chain in immature dendritic cells [18]. Therefore, investigating the changes in the expression of invariant chain and localization of MHC proteins in the cell under such circumstances might shed light on such features. In the future, it would be of advantage to explore the features of CD1d in the plasma membrane with super-resolution microscopes. These microscopes, like stimulated emission depletion microscopy and near-field scanning optical microscope, are capable of imaging structures beyond the diffraction limit providing resolution below sub 100 nm, therefore, it can provide far more insights into the dynamics and nature of molecular interactions than a conventional confocal microscope. Especially, fluorescence correlation spectroscopy with the aid of these microscopies would be able to dissect the dynamic relationship between CD1d and GM<sub>1</sub> gangliosides or rafts. We believe that elucidating these molecular features of CD1d proteins on the plasma membrane would help us understand the potential ways how CD1d mediated immune pathways could be regulated for therapeutic purpose.

Supplementary data to this article can be found online at <http://dx.doi.org/10.1016/j.bbagen.2013.10.030>.

## Acknowledgements

We would like to thank the support of research grants from the Hungarian Scientific Research Fund (NK 101337); the European Commission grants (LSHC-CT-2005-018914) -ATTACK, MCRTN-CT-2006-036946-2 (IMMUNANOMAP), OTKA NK Research Grant 101337, the New Hungary Development Plan co-financed by the European Social Fund and the European Regional Development Fund (TÁMOP-4.2.2.A-11/1/KONV-2012-0025, TÁMOP-4.2.2-08/1-2008-0019, TÁMOP-4.2.2.A-11/1/KONV-2012-0036 and TÁMOP-4.2.1/B-09/1/KONV-2010-007). We also appreciate TÁMOP-4.2.2/B-10/1-2010-0024 Predoctoral fellowship for supporting Dilip Shrestha. MAE was supported by NIH grants CA143748 and CA170194. Lastly, we thank Anita Sárvári from the Department of Biochemistry and Molecular Biology, University of Debrecen for generously arranging and providing PBMC samples and Adrienn Bagosi for her excellent technical assistance.

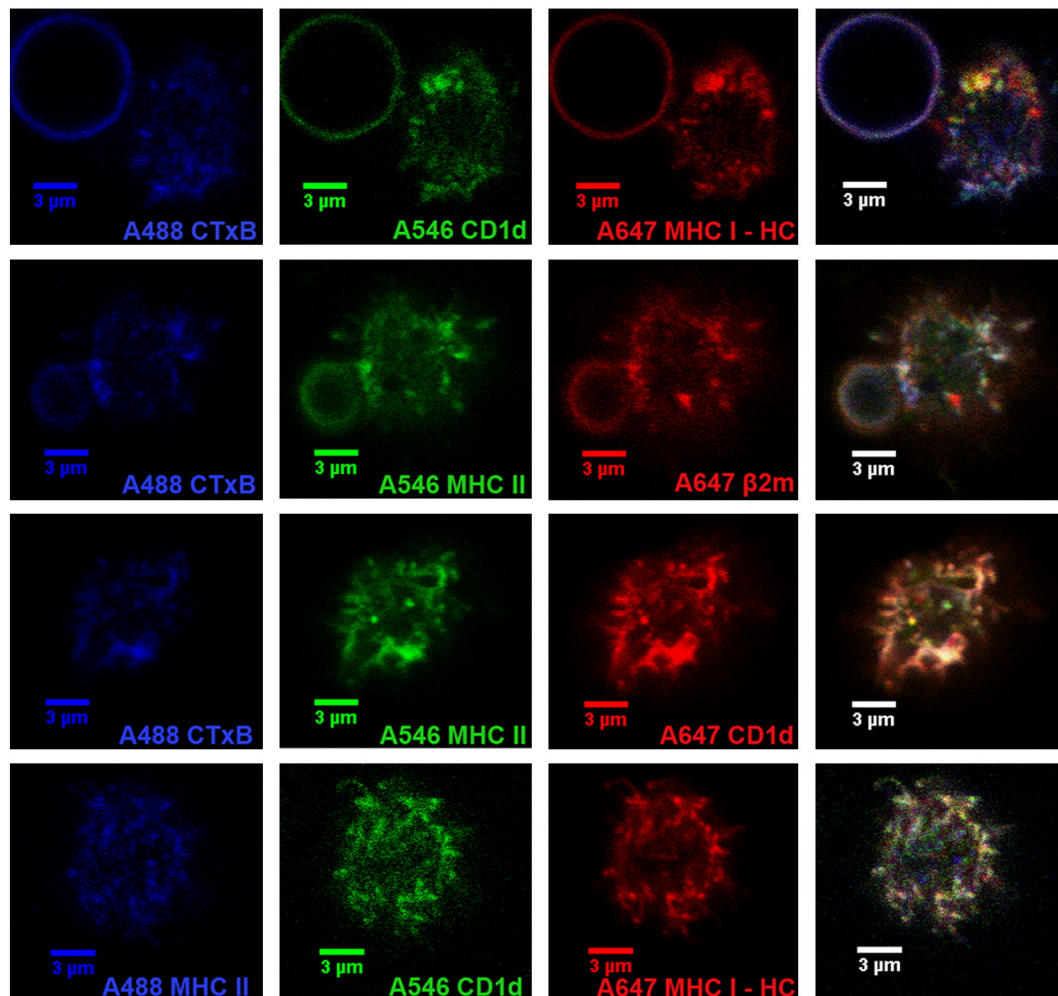


**Fig. 9.** Triple color labeling experiment: Three molecules from MHC I-HC,  $\beta_2m$ , MHC II, CD1d and GM<sub>1</sub> subunit molecules were labeled simultaneously in similar ways as described in the Materials and methods section. Once prepared, the fixed samples were washed thoroughly, thereafter; the cells were laid on poly-lysine (0.1 mg/ml) coated ibidi chambers. Receptors were then imaged from the top of the membrane using confocal microscope. Specific dyes were used for individual receptors, which are indicated at the right bottom of each image. The last column represents the superimposed image of all the three other columns. Emission from Alexa 488, Alexa 546 and Alexa 647 dyes were collected through 505/550 nm BP filter, 560/615 nm BP filter and 650 LP filter respectively.

## References

- [1] S. Porcelli, M.B. Brenner, J.L. Greenstein, S.P. Balk, C. Terhorst, P.A. Bleicher, Recognition of cluster of differentiation 1 antigens by human CD4–CD8–cytolytic T lymphocytes, *Nature* 341 (1989) 447–450.
- [2] E.M. Beckman, S.A. Porcelli, C.T. Morita, S.M. Behar, S.T. Furlong, M.B. Brenner, Recognition of a lipid antigen by CD1-restricted alpha beta+ T cells, *Nature* 372 (1994) 691–694.
- [3] L. Mori, G. De Libero, T cells specific for lipid antigens, *Immunol. Res.* 53 (2012) 191–199.
- [4] X. Chen, X. Wang, J.M. Keaton, F. Reddington, P.A. Illarionov, G.S. Besra, J.E. Gumperz, Distinct endosomal trafficking requirements for presentation of autoantigens and exogenous lipids by human CD1d molecules, *J. Immunol.* 178 (2007) 6181–6190.
- [5] C.Y. Yu, C. Milstein, A physical map linking the five CD1 human thymocyte differentiation antigen genes, *EMBO J.* 8 (1989) 3727–3732.
- [6] M. Sugita, D.C. Barral, M.B. Brenner, Pathways of CD1 and lipid antigen delivery, trafficking, processing, loading, and presentation, *Curr. Top. Microbiol. Immunol.* 314 (2007) 143–164.
- [7] M. Brigl, M.B. Brenner, CD1: antigen presentation and T cell function, *Annu. Rev. Immunol.* 22 (2004) 817–890.
- [8] C. Gelin, I. Sloma, D. Charron, N. Mooney, Regulation of MHC II and CD1 antigen presentation: from ubiquity to security, *J. Leukoc. Biol.* 85 (2009) 215–224.
- [9] Q. Zhang, R.D. Salter, Distinct patterns of folding and interactions with calnexin and calreticulin in human class I MHC proteins with altered N-glycosylation, *J. Immunol.* 160 (1998) 831–837.
- [10] S.J. Kang, P. Cresswell, Calnexin, calreticulin, and ERp57 cooperate in disulfide bond formation in human CD1d heavy chain, *J. Biol. Chem.* 277 (2002) 44838–44844.
- [11] H.S. Kim, J. Garcia, M. Exley, K.W. Johnson, S.P. Balk, R.S. Blumberg, Biochemical characterization of CD1d expression in the absence of beta2-microglobulin, *J. Biol. Chem.* 274 (1999) 9289–9295.
- [12] V. O'Reilly, S.G. Zeng, G. Bricard, A. Atzberger, A.E. Hogan, J. Jackson, C. Feighery, S.A. Porcelli, D.G. Doherty, Distinct and overlapping effector functions of expanded human CD4+, CD8alpha+ and CD4–CD8alpha- invariant natural killer T cells, *PLoS One* 6 (2011) e28648.
- [13] Y.J. Chang, J.R. Huang, Y.C. Tsai, J.T. Hung, D. Wu, M. Fujio, C.H. Wong, A.L. Yu, Potent immune-modulating and anticancer effects of NKT cell stimulatory glycolipids, *Proc. Natl. Acad. Sci. U. S. A.* 104 (2007) 10299–10304.
- [14] M. Sugita, R.M. Jackman, E. van Donselaar, S.M. Behar, R.A. Rogers, P.J. Peters, M.B. Brenner, S.A. Porcelli, Cytoplasmic tail-dependent localization of CD1b antigen-presenting molecules to MHCs, *Science* 273 (1996) 349–352.
- [15] M. Cernadas, M. Cavallari, G. Watts, L. Mori, G. De Libero, M.B. Brenner, Early recycling compartment trafficking of CD1a is essential for its intersection and presentation of lipid antigens, *J. Immunol.* 184 (2010) 1235–1241.
- [16] D.C. Barral, M. Cavallari, P.J. McCormick, S. Garg, A.I. Magee, J.S. Bonifacino, G. De Libero, M.B. Brenner, CD1a and MHC class I follow a similar endocytic recycling pathway, *Traffic* 9 (2008) 1446–1457.
- [17] K.C. Roy, I. Maricic, A. Khurana, T.R. Smith, R.C. Halder, V. Kumar, Involvement of secretory and endosomal compartments in presentation of an exogenous self-glycolipid to type II NKT cells, *J. Immunol.* 180 (2008) 2942–2950.
- [18] I. Sloma, M.T. Zilber, T. Vasselon, N. Setterblad, M. Cavallari, L. Mori, G. De Libero, D. Charron, N. Mooney, C. Gelin, Regulation of CD1a surface expression and antigen presentation by invariant chain and lipid rafts, *J. Immunol.* 180 (2008) 980–987.
- [19] Y. Sagiv, L. Bai, D.G. Wei, R. Agami, P.B. Savage, L. Teyton, A. Bendelac, A distal effect of microsomal triglyceride transfer protein deficiency on the lysosomal recycling of CD1d, *J. Exp. Med.* 204 (2007) 921–928.
- [20] A.O. Speak, N. Platt, M. Salio, D.T. Vruchte, D.A. Smith, D. Shepherd, N. Veerapen, G. Besra, N.M. Yanjanin, L. Simmons, J. Imrie, J.E. Wraith, R. Lachmann, R. Hartung, H. Runz, E. Mengel, M. Beck, C.J. Hendriks, F.D. Porter, V. Cerundolo, F.M. Platt, Invariant Natural Killer T cells are not affected by lysosomal storage in patients with Niemann–Pick disease type C, *Eur. J. Immunol.* (2012).

Q4

- [21] A.P. Lawton, T.I. Grigozy, L. Brossay, B. Pei, A. Khurana, D. Martin, T. Zhu, K. Spate, M. Ozga, S. Honing, O. Bakke, M. Kronenberg, The mouse CD1d cytoplasmic tail mediates CD1d trafficking and antigen presentation by adaptor protein 3-dependent and -independent mechanisms, *J. Immunol.* 174 (2005) 3179–3186.
- [22] T.S. Devera, L.M. Aye, G.A. Lang, S.K. Joshi, J.D. Ballard, M.L. Lang, CD1d-dependent B-cell help by NK-like T cells leads to enhanced and sustained production of *Bacillus anthracis* lethal toxin-neutralizing antibodies, *Infect. Immun.* 78 (2010) 1610–1617.
- [23] E. Tonti, G. Galli, C. Malzone, S. Abrignani, G. Casorati, P. Dellabona, NKT-cell help to B lymphocytes can occur independently of cognate interaction, *Blood* 113 (2009) 370–376.
- [24] A. Bosma, A. Abdel-Gadir, D.A. Isenberg, E.C. Jury, C. Mauri, Lipid-antigen presentation by CD1d(+) B cells is essential for the maintenance of invariant natural killer T cells, *Immunity* 36 (2012) 477–490.
- [25] S.J. Kang, P. Cresswell, Regulation of intracellular trafficking of human CD1d by association with MHC class II molecules, *EMBO J.* 21 (2002) 1650–1660.
- [26] S.P. Balk, S. Burke, J.E. Polischuk, M.E. Frantz, L. Yang, S. Porcelli, S.P. Colgan, R.S. Blumberg, Beta 2-microglobulin-independent MHC class Ib molecule expressed by human intestinal epithelium, *Science* 265 (1994) 259–262.
- [27] J. Jayawardena-Wolf, K. Benlagha, Y.H. Chiu, R. Mehr, A. Bendelac, CD1d endosomal trafficking is independently regulated by an intrinsic CD1d-encoded tyrosine motif and by the invariant chain, *Immunity* 15 (2001) 897–908.
- [28] Y.K. Park, J.W. Lee, Y.G. Ko, S. Hong, S.H. Park, Lipid rafts are required for efficient signal transduction by CD1d, *Biochem. Biophys. Res. Commun.* 327 (2005) 1143–1154.
- [29] S. Karmakar, J. Paul, T. De, Leishmania donovani glycosphingolipid facilitates antigen presentation by inducing relocation of CD1d into lipid rafts in infected macrophages, *Eur. J. Immunol.* 41 (2011) 1376–1387.
- [30] W. Peng, C. Martaresche, N. Escande-Beillard, O. Cedile, A. Reynier-Vigouroux, J. Boucraut, Influence of lipid rafts on CD1d presentation by dendritic cells, *Mol. Membr. Biol.* 24 (2007) 475–484.
- [31] G.A. Lang, S.D. Maltsev, G.S. Besra, M.L. Lang, Presentation of alpha-galactosylceramide by murine CD1d to natural killer T cells is facilitated by plasma membrane glycolipid rafts, *Immunology* 112 (2004) 386–396.
- [32] J. Szollosi, S. Damjanovich, M. Balazs, P. Nagy, L. Tron, M.J. Fulwyler, F.M. Brodsky, Physical association between MHC class I and class II molecules detected on the cell surface by flow cytometric energy transfer, *J. Immunol.* 143 (1989) 208–213.
- [33] A. Jenéi, S. Varga, L. Bene, L. Matyus, A. Bodnar, Z. Bacso, C. Pieri, R. Gaspar Jr., T. Farkas, S. Damjanovich, HLA class I and II antigens are partially co-clustered in the plasma membrane of human lymphoblastoid cells, *Proc. Natl. Acad. Sci. U. S. A.* 94 (1997) 7269–7274.
- [34] Z. Bacso, L. Bene, L. Damjanovich, S. Damjanovich, INF-gamma rearranges membrane topography of MHC-I and ICAM-1 in colon carcinoma cells, *Biochem. Biophys. Res. Commun.* 290 (2002) 635–640.
- [35] L. Bene, Z. Kanyari, A. Bodnar, J. Kappelmayer, T.A. Waldmann, G. Vamosi, L. Damjanovich, Colorectal carcinoma rearranges cell surface protein topology and density in CD4+ T cells, *Biochem. Biophys. Res. Commun.* 361 (2007) 202–207.
- [36] J. Szollosi, V. Horejsi, L. Bene, P. Angelisova, S. Damjanovich, Supramolecular complexes of MHC class I, MHC class II, CD20, and tetraspan molecules (CD53, CD81, and CD82) at the surface of a B cell line JY, *J. Immunol.* 157 (1996) 2939–2946.
- [37] J. Zemmour, A.M. Little, D.J. Schendel, P. Parham, The HLA-A, B “negative” mutant cell line C1R expresses a novel HLA-B35 allele, which also has a point mutation in the translation initiation codon, *J. Immunol.* 148 (1992) 1941–1948.
- [38] M. Exley, J. Garcia, S.P. Balk, S. Porcelli, Requirements for CD1d recognition by human invariant Valpha24+ CD4–CD8–T cells, *J. Exp. Med.* 186 (1997) 109–120.
- [39] C.J. Barnstable, W.F. Bodmer, G. Brown, G. Galfre, C. Milstein, A.F. Williams, A. Ziegler, Production of monoclonal antibodies to group A erythrocytes HLA and other human cell surface antigens—new tools for genetic analysis, *Cell* 14 (1978) 9–20.
- [40] M. Gauster, A. Blaschitz, G. Dohr, Monoclonal antibody HC10 does not bind HLA-G, *Rheumatology (Oxford)* 46 (2007) 892–893.
- [41] F. Perosa, G. Luccarelli, M. Prete, E. Favoino, S. Ferrone, F. Dammacco, Beta 2-microglobulin-free HLA class I heavy chain epitope mimicry by monoclonal antibody HC-10-specific peptide, *J. Immunol.* 171 (2003) 1918–1926.
- [42] N.J. Stam, H. Spits, H.L. Ploegh, Monoclonal antibodies raised against denatured HLA-B locus heavy chains permit biochemical characterization of certain HLA-C locus products, *J. Immunol.* 137 (1986) 2299–2306.
- [43] N.J. Stam, T.M. Vroom, P.J. Peters, E.B. Pastoors, H.L. Ploegh, HLA-A- and HLA-B-specific monoclonal antibodies reactive with free heavy chains in western blots, in formalin-fixed, paraffin-embedded tissue sections and in cryo-immuno-electron microscopy, *Int. Immunol.* 2 (1990) 113–125.
- [44] L.A. Lampson, C.A. Fisher, J.P. Whelan, Striking paucity of HLA-A, B, C and beta 2-microglobulin on human neuroblastoma cell lines, *J. Immunol.* 130 (1983) 2471–2478.
- [45] P.A. Robbins, E.L. Evans, A.H. Ding, N.L. Warner, F.M. Brodsky, Monoclonal antibodies that distinguish between class II antigens (HLA-DP, DQ, and DR) in 14 haplotypes, *Hum. Immunol.* 18 (1987) 301–313.
- [46] C. Schneider, R. Sutherland, R. Newman, M. Greaves, Structural features of the cell surface receptor for transferrin that is recognized by the monoclonal antibody OKT9, *J. Biol. Chem.* 257 (1982) 8516–8522.
- [47] M. Exley, J. Garcia, S.B. Wilson, F. Spada, D. Gerdes, S.M. Tahir, K.T. Patton, R.S. Blumberg, S. Porcelli, A. Chott, S.P. Balk, CD1d structure and regulation on human thymocytes, peripheral blood T cells B cells and monocytes, *Immunology* 100 (2000) 37–47.
- [48] V. Horejsi, P. Angelisova, V. Bazil, H. Kristofova, S. Stoyanov, I. Stefanova, P. Hausner, M. Vosecky, I. Hilgert, Monoclonal antibodies against human leucocyte antigens. II. Antibodies against CD45 (T200), CD3 (T3), CD43, CD10 (CALLA), transferrin receptor (T9), a novel broadly expressed 18-kDa antigen (MEM-43) and a novel antigen of restricted expression (MEM-74), *Folia Biol. (Praha)* 34 (1988) 23–34.
- [49] G. Vereb, J. Matko, G. Vamosi, S.M. Ibrahim, E. Magyar, S. Varga, J. Szollosi, A. Jenéi, R. Gaspar Jr., T.A. Waldmann, S. Damjanovich, Cholesterol-dependent clustering of IL-2Ralpha and its colocalization with HLA and CD48 on T lymphoma cells suggest their functional association with lipid rafts, *Proc. Natl. Acad. Sci. U. S. A.* 97 (2000) 6013–6018.
- [50] G. Vereb, J. Szöllösi, S. Damjanovich, J. Matkó, Exploring membrane microdomains and functional protein clustering in live cells with flow and image cytometric methods, Kluwer Academic / Plenum Publishers, New York, 2004.
- [51] G. Szentesi, G. Horvath, I. Bori, G. Vamosi, J. Szollosi, R. Gaspar, S. Damjanovich, A. Jenéi, L. Matyus, Computer program for determining fluorescence resonance energy transfer efficiency from flow cytometric data on a cell-by-cell basis, *Comput. Methods Programs Biomed.* 75 (2004) 201–211.
- [52] I. Gombos, Z. Bacso, C. Detre, H. Nagy, K. Goda, M. Andrasfalvy, G. Szabo, J. Matko, Cholesterol sensitivity of detergent resistance: a rapid flow cytometric test for detecting constitutive or induced raft association of membrane proteins, *Cytometry A* 61 (2004) 117–126.
- [53] L. Bene, A. Bodnar, S. Damjanovich, G. Vamosi, Z. Bacso, J. Aradi, A. Berta, J. Damjanovich, Membrane topography of HLA I, HLA II, and ICAM-1 is affected by INF-gamma in lipid rafts of uveal melanomas, *Biochem. Biophys. Res. Commun.* 322 (2004) 678–683.
- [54] R. Knorr, C. Karacsonyi, R. Lindner, Endocytosis of MHC molecules by distinct membrane rafts, *J. Cell Sci.* 122 (2009) 1584–1594.
- [55] H.A. Anderson, E.M. Hiltbold, P.A. Roche, Concentration of MHC class II molecules in lipid rafts facilitates antigen presentation, *Nat. Immunol.* 1 (2000) 156–162.
- [56] L. Damjanovich, J. Volko, A. Forgacs, W. Hohenberger, L. Bene, Crohn's disease alters MHC-rafts in CD4(+) T-cells, *Cytometry A* 81 (2012) 149–164.
- [57] M. Bouillon, Y. El Fakhry, J. Girouard, H. Khalil, J. Thibodeau, W. Mourad, Lipid raft-dependent and -independent signaling through HLA-DR molecules, *J. Biol. Chem.* 278 (2003) 7099–7107.
- [58] D. Lingwood, K. Simons, Lipid rafts as a membrane-organizing principle, *Science* 327 (2010) 46–50.
- [59] E.S. Istvan, J. Deisenhofer, Structural mechanism for statin inhibition of HMG-CoA reductase, *Science* 292 (2001) 1160–1164.
- [60] R. Zidovetzki, I. Levitan, Use of cyclodextrins to manipulate plasma membrane cholesterol content: evidence, misconceptions and control strategies, *Biochim. Biophys. Acta* 1768 (2007) 1311–1324.
- [61] M.A. Khan, R.M. Gallo, G.J. Renukaradhya, W. Du, J. Gervay-Hague, R.R. Brutkiewicz, Statins impair CD1d-mediated antigen presentation through the inhibition of prenylation, *J. Immunol.* 182 (2009) 4744–4750.
- [62] C. Lagaudriere-Gesbert, S. Lebel-Binay, E. Wiertz, H.L. Ploegh, D. Fradelizi, H. Conjeaud, The tetraspanin protein CD82 associates with both free HLA class I heavy chain and heterodimeric beta 2-microglobulin complexes, *J. Immunol.* 158 (1997) 2790–2797.
- [63] H. de la Fuente, M. Mittelbrunn, L. Sanchez-Martin, M. Vicente-Manzanares, A. Lamana, R. Pardi, C. Cabanas, F. Sanchez-Madrid, Synaptic clusters of MHC class II molecules induced on DCs by adhesion molecule-mediated initial T-cell scanning, *Mol. Biol. Cell* 16 (2005) 3314–3322.
- [64] E.M. Hiltbold, N.J. Poloso, P.A. Roche, MHC class II-peptide complexes and APC lipid rafts accumulate at the immunological synapse, *J. Immunol.* 170 (2003) 1329–1338.
- [65] L. Damjanovich, J. Volko, A. Forgacs, W. Hohenberger, L. Bene, Crohn's disease alters MHC-rafts in CD4+ T-cells, *Cytometry A* 81 (2012) 149–164.
- [66] N. Setterblad, C. Roucard, C. Bocaccio, J.P. Abastado, D. Charron, N. Mooney, Composition of MHC class II-enriched lipid microdomains is modified during maturation of primary dendritic cells, *J. Leukoc. Biol.* 74 (2003) 40–48.
- [67] K. Somnay-Wadgaonkar, A. Nusrat, H.S. Kim, W.P. Canchis, S.P. Balk, S.P. Colgan, R.S. Blumberg, Immunolocalization of CD1d in human intestinal epithelial cells and identification of a beta2-microglobulin-associated form, *Int. Immunol.* 11 (1999) 383–392.
- [68] J. Liu, D. Shaji, S. Cho, W. Du, J. Gervay-Hague, R.R. Brutkiewicz, A threonine-based targeting signal in the human CD1d cytoplasmic tail controls its functional expression, *J. Immunol.* 184 (2010) 4973–4981.
- [69] M. Amano, N. Baumgarth, M.D. Dick, L. Brossay, M. Kronenberg, L.A. Herzenberg, S. Strober, CD1 expression defines subsets of follicular and marginal zone B cells in the spleen: beta 2-microglobulin-dependent and independent forms, *J. Immunol.* 161 (1998) 1710–1717.
- [70] M. Duman, M. Pfleger, R. Zhu, C. Rankl, L.A. Chtcheglova, I. Neundlinger, B.L. Bozna, B. Mayer, M. Salio, D. Shepherd, P. Polzella, M. Moertelmaier, G. Kada, A. Ebner, M. Dieudonne, G.J. Schutz, V. Cerundolo, F. Kienberger, P. Hinterdorfer, Improved localization of cellular membrane receptors using combined fluorescence microscopy and simultaneous topography and recognition imaging, *Nanotechnology* 21 (2010) 115504.
- [71] M. Duman, L.A. Chtcheglova, R. Zhu, B.L. Bozna, P. Polzella, V. Cerundolo, P. Hinterdorfer, Nanomapping of CD1d-glycolipid complexes on THP1 cells by using simultaneous topography and recognition imaging, *J. Mol. Recognit.* 26 (2013) 408–414.
- [72] R. Ghittoni, G. Napolitani, D. Benati, C. Olivieri, L. Patrussi, F. Laghi Pasini, A. Lanzavecchia, C.T. Baldari, Simvastatin inhibits the MHC class II pathway of antigen presentation by impairing Ras superfamily GTPases, *Eur. J. Immunol.* 36 (2006) 2885–2893.
- [73] B.M. Maher, T.N. Dhonnchu, J.P. Burke, A. Soo, A.E. Wood, R.W. Watson, Statins alter neutrophil migration by modulating cellular Rho activity—a potential mechanism for statins-mediated pleiotropic effects? *J. Leukoc. Biol.* 85 (2009) 186–193.
- [74] A.M. deCathelineau, G.M. Bokoch, Inactivation of rho GTPases by statins attenuates anthrax lethal toxin activity, *Infect. Immun.* 77 (2009) 348–359.
- [75] G. Martin, H. Duez, C. Blanquart, V. Berezowski, P. Poulain, J.C. Fruchart, J. Najib-Fruchart, C. Glineur, B. Staels, Statin-induced inhibition of the Rho-signaling

- 971 pathway activates PPARalpha and induces HDL apoA-I, *J. Clin. Invest.* 107 (2001) 989  
 972 1423–1432. 990
- 973 [76] R. Ghittoni, L. Patrussi, K. Pirozzi, M. Pellegrini, P.E. Lazzerini, P.L. Capecchi, F.L. 991  
 974 Pasini, C.T. Baldari, Simvastatin inhibits T-cell activation by selectively impairing 992  
 975 the function of Ras superfamily GTPases, *FASEB J.* 19 (2005) 605–607. 993
- 976 [77] M. Copaja, D. Venegas, P. Aranguiz, J. Canales, R. Vivar, Y. Avalos, L. Garcia, M. Chiong, 994  
 977 I. Olmedo, M. Catalan, L. Leyton, S. Lavandero, G. Diaz-Araya, Simvastatin disrupts 995  
 978 cytoskeleton and decreases cardiac fibroblast adhesion, migration and viability, *Toxi-* 996  
 979 *cology* 294 (2012) 42–49. 997
- 980 [78] M. Pozo, R. de Nicolas, J. Egido, J. Gonzalez-Cabrero, Simvastatin inhibits the migra- 998  
 981 tion and adhesion of monocytic cells and disorganizes the cytoskeleton of activated 999  
 982 endothelial cells, *Eur. J. Pharmacol.* 548 (2006) 53–63. 1000
- 983 [79] R.M. Gallo, M.A. Khan, J. Shi, R. Kapur, L. Wei, J.C. Bailey, J. Liu, R.R. Brutkiewicz, Reg- 1001  
 984 ulation of the actin cytoskeleton by Rho kinase controls antigen presentation by 1002  
 985 CD1d, *J. Immunol.* 189 (2012) 1689–1698. 1003
- 986 [80] J.S. Im, P. Arora, G. Bricard, A. Molano, M.M. Venkataswamy, I. Baine, E.S. Jerud, M.F. 1004  
 987 Goldberg, A. Baena, K.O. Yu, R.M. Ndonge, A.R. Howell, W. Yuan, P. Cresswell, Y.T. 1005  
 988 Chang, P.A. Illarionov, G.S. Besra, S.A. Porcelli, Kinetics and cellular site of glycolipid 1006  
 loading control the outcome of natural killer T cell activation, *Immunity* 30 (2009) 1007  
 888–898. 990
- [81] D. Locke, J. Liu, A.L. Harris, Lipid rafts prepared by different methods contain differ- 991  
 ent connexin channels, but gap junctions are not lipid rafts, *Biochemistry* 44 (2005) 992  
 13027–13042. 993
- [82] K. Roper, D. Corbeil, W.B. Huttner, Retention of prominin in microvilli reveals distinct 994  
 cholesterol-based lipid micro-domains in the apical plasma membrane, *Nat.* 995  
*Cell Biol.* 2 (2000) 582–592. 996
- [83] J.F. Frisz, H.A. Klitzing, K. Lou, I.D. Hutcheon, P.K. Weber, J. Zimmerberg, M.L. Kraft, 997  
 Sphingolipid domains in the plasma membranes of fibroblasts are not enriched 998  
 with cholesterol, *J. Biol. Chem.* 288 (2013) 16855–16861. 999
- [84] E.K. Bikoff, L.Y. Huang, V. Episkopou, J. van Meerwijk, R.N. Germain, E.J. Robertson, 1000  
 Defective major histocompatibility complex class II assembly, transport, peptide ac- 1001  
 quisition, and CD4+ T cell selection in mice lacking invariant chain expression, *J.* 1002  
*Exp. Med.* 177 (1993) 1699–1712. 1003
- [85] E.A. Elliott, J.R. Drake, S. Amigorena, J. Elsemore, P. Webster, I. Mellman, R.A. Flavell, 1004  
 The invariant chain is required for intracellular transport and function of major his- 1005  
 tocompatibility complex class II molecules, *J. Exp. Med.* 179 (1994) 681–694. 1006  
 1007

UNCORRECTED PROOF